Heavy metal ATPases from archaeabacteria to plants

by

María José Orofino

A Thesis

Submitted to the Faculty

of the

WORCESTER POLYTECHNIC INSTITUTE

in partial fulfillment of the requirements for the

Degree of Master of Science

in

Biochemistry

_____

May 2006

APPROVED:

_____

Dr. José M. Argüello, Major Advisor

_____

Dr. James W. Pavlik, Head of Department

ACKNOWLEDGEMENTS

ABSTRACT

P_{IB}-ATPases are membrane proteins that transport heavy metal ions across biological membranes upon ATP-hydrolysis. These enzymes contribute to metal homeostasis in archaeal, prokaryotic and eukaryotic cells. Typically, most P_{IB}-ATPases have eight transmembrane segments, one or more metal binding domains in the cytoplasmic N-terminal region and a series of amino acids conserved in all the members of this family. By sequence homology analysis, the metal specificity for most ATPases has been predicted. Here, we report studies on P_{IB}-ATPases from different organisms.

The first part of this work focuses in a group of ATPases from *Arabidopsis thaliana* plants. Transcription levels of HMA3, 4 and 8 were analyzed in different plant organs and in seedlings upon metal exposure. Tissue specificity was studied for HMA8 by generation of transgenic plants carrying a reporter gene downstream its promoter region. Attempts to determine metal specificity of proteins expressed in yeast cells were performed. Finally, in order to study the effects of removing the genes products from the plants, HMA4 and 8 mutant plants were identified.

The second part describes a novel Pb-transport ATPase from a thermophilic archaeabacterium, *Aeropyrum pernix*. This enzyme is predicted to have only six transmembrane segments, no regulatory metal binding domains and unusual metal specificity. PbTP was cloned, expressed in *Escherichia coli* and partially purified. The enzyme retained its thermophilicity characteristics when isolated from its native lipid environment. The metal dependent ATPase activity was determined in the presence of different metals at 75ºC. The enzyme was highly activated by Pb^{2+} (Vmax: 23.6 µmol Pi/mg/h) and to a lesser extent by Zn^{2+}, Hg^{2+} and Cd^{2+}. Lead interacts with PbTP with high apparent affinity ($K_{1/2}$: 4.6 µM). The enzymatic ATP hydrolysis was independent of cysteine or glutathione, suggesting direct interaction of the metal ions with the transmembrane transport sites.

iii

TABLE OF CONTENTS

INTRODUCTION

Heavy metal homeostasis

Metal ions such as Cu^{2+}, Co^{2+}, Zn^{2+}, Fe^{2+}, Ni^{2+} and Mn^{2+} represent essential elements for living organisms. These ions are constituents of diverse protein molecules and are required in trace amounts. For example, Cu^{2+} is required for enzymes such as superoxide dismutase, cytochrome c oxidase and plastocyanin; Zn^{2+} acts as a cofactor of a number of enzymes and is also found in structural domains of several proteins (i.e. Zn-finger domains) [1-3]. However, high concentrations of these metals as well as non-essential ions such as Cd^{2+}, Ag^+ or Pb^{2+} have toxic effects in the cell. This toxicity is conferred by the ability of some metals to form strong bonds with the side chains of amino acids (for instance, with S and N atoms in Cys and His), or to cause oxidative damage by generation of reactive oxygen species [1, 2]. Cells have evolved a series of metal transport processes that prevent accumulation of metal ions in the free form and simultaneously ensure the delivery of the ions to metalloproteins. Metallochaperones and transmembrane transporters are involved in these processes [1, 4-15].

Chelation and trafficking of heavy metal ions

Metallochaperones mediate the intracellular metal ions distribution by binding the metal and delivering it to specific target proteins. Chaperones form a family of soluble, low molecular weight (~7 kDa) cytosolic proteins with key metal binding cysteines. It has been proposed that, at least in yeast cells, there are no free copper ions [16], suggesting that the cytosolic levels of this metal are tightly regulated. Cu^+ chaperones have been identified both in eukaryotes and prokaryotes. These can be classified in three main groups based on which protein they deliver the ion to: superoxide dismutase, cytochrome oxidases or P-type ATPases. For example, in *Saccharomyces cerevisiae* CCS delivers Cu^+ to Cu/Zn-superoxide dismutase [16-18]; Cox17 directs Cu^+ to the mitochondria activating cytochrome oxidase [19, 20]; and Atx1 delivers the metal to a P-type ATPase (CCC2) in Golgi [21]. The Atx1 human homolog, HAH1, also delivers the ions to the secretory system [22]. CCH and AtCox17 appear to be Cu-chaperones in *Arabidopsis thaliana* [23, 24]. The prokaryotic homolog of Atx1, CopZ, has been

identified in *Enterococcus hirae* and *Bacilus subtilis* [25, 26]. Putative Atx1-like copper chaperones are also present in archaeabacteria [27].

Several solution or crystal structures for apo- and metal-bound chaperones are available [28-34]. All the Atx1-like chaperones show "ferredoxin-like" secondary structures ($\beta\alpha\beta\beta\alpha\beta$) [29, 31, 33-35], containing a "MXCXXC" metal binding domain [29, 33, 36] which can bind copper with an stoichiometry of one metal ion per chaperone molecule [21, 32, 37, 38]. Cu transfer from metallochaperones to metal binding domains of target proteins and in some cases their interaction have been reported for HAH1, Atx1 and the bacterial CopZ [39-51].

Transport of heavy metals across biological membranes

A number of membrane proteins play a key role in heavy metal homeostasis by transporting the ions across the cell membrane. ABC (<u>A</u>TP <u>B</u>inding <u>C</u>assette), CDF (<u>C</u>ation <u>D</u>iffusion <u>F</u>acilitator), Nramp (<u>N</u>atural resistance associated <u>m</u>acrophage proteins), ZIP (<u>Z</u>inc Regulated Transporter/<u>I</u>ron Regulated Transporter related <u>P</u>roteins) and P_{IB}-ATPases are among these gene families that transport heavy metal ions.

The *ABC ATPases* constitute a superfamily with a wide range of substrate specificity that includes ions, antibiotics, sugars, peptides and lipids [14]. There is evidence of Cd-phytochelatin complexes transport into yeast and plant vacuoles mediated by ABC ATPases [52, 53]; also, some ABC proteins were suggested to participate in plant iron homeostasis [54]. Members of the *CDF* family have been identified in bacteria, archaea and eukaryotes. These 6 transmembrane fragments proteins transport Zn^{2+}, Co^{2+} and Cd^{2+}, and a role in Zn^{2+} vacuolar sequestration has been suggested for plant representatives [3, 14, 55-57]. Proteins of the *ZIP* family are involved in Fe^{2+}, Zn^{2+}, Ni^{2+}, Mn^{2+} and Cd^{2+} transport [3, 58-63]. The *Nramp* proteins have been involved in transport of Fe^{2+}, Cu^{2+}, Co^{2+}, Mn^{2+} and Cd^{2+} ions in prokaryotes and eukaryotes [14, 56, 64-68].

P_{IB}-ATPases (also referred as *heavy metal ATPases*) are members of the P-type ATPases superfamily, a large group of ATP-driven pumps involved in the transport of various cations across biomembranes. P-type ATPases have been identified in archaea, prokaryotes and eukaryotes, and some of them have been thoroughly studied [69-75]. Members of the P-type ATPase superfamily have been grouped in 5 subfamilies (I to V)

2

based on substrate specificity [76, 77] (http://www.biobase.dk/~axe/Patbase.html). For instance, P_{II}-ATPases include the well-characterized sarcoplasmic reticulum Ca^{2+}-ATPase, Na^+/K^+-ATPase, H^+-ATPases and H^+/K^+-ATPase [77].

A common feature to all P-type ATPases is the formation of a phosphorylated intermediate during their catalytic cycle; and the existence of at least two conformations, E_1 and E_2, which are associated with ion translocation. The phosphorylation occurs invariably in the aspartic acid residue present in the cytoplasmic DKTGT consensus sequence. There is evidence supporting that P_{IB}-ATPases enzymatic cycle is similar to the cycle undergone by the P_{II}-ATPases [78-82]. The proposed catalytic cycle for a heavy metal ATPase is illustrated in Fig. 1. Briefly, ATP-Mg^{2+} are bound to the enzyme in E_1 state, the intracellular metal ion binds to the protein and the phosphorylation occurs. The E_1 conformational state has intracellular facing cation binding sites and exhibits high affinity for the metal ion and ATP. The E_1P form can be dephosphorylated by ADP in the reverse reaction. In the forward reaction, ADP is released and the metal ions are now occluded. The ions leave the protein in the extracellular face upon a new conformational change ($E_2.P$). The protein is then dephosphorylated. Upon ATP binding to a low affinity binding site the enzyme returns to the E_1 state initiating the cycle again [70, 80]. Another common feature to all the P-type ATPases is the inhibition by vanadate. This compound binds to the enzyme in the E_2 conformation, arresting the cycle in an $E_2.$vanadate form [83].
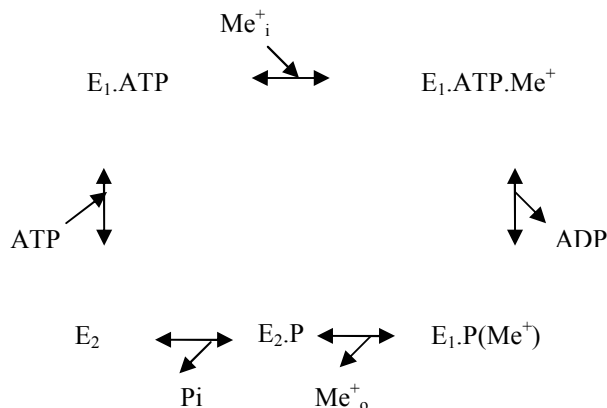
Fig. 1. Scheme of P_{IB}-ATPases catalytic cycle. E_1 and E_2 are the two conformational forms of the enzyme. Subscripts i and o represent intracellular and extracellular respectively; occluded ions are shown in parenthesis. Me^+: metal ion.

P_{IB}-ATPases share the mentioned features of P-Type ATPases and they also show novel ones: (a) P_{IB}-ATPases contain six to eight transmembrane fragments (TMs); (b) the sixth TM has a CPC, CPS, SPC, TPC or CPH ("xPx sequence") upstream the phosphorylation site (**D**KTGT); and (c) a variable number of putative metal binding domains (CXXC or His-rich) in the amino terminal region [9, 84], although in some P_{IB}-ATPases these domains are in the C-terminus or completely absent. A scheme of the general topology of P_{IB}-ATPases is shown in Fig. 2.
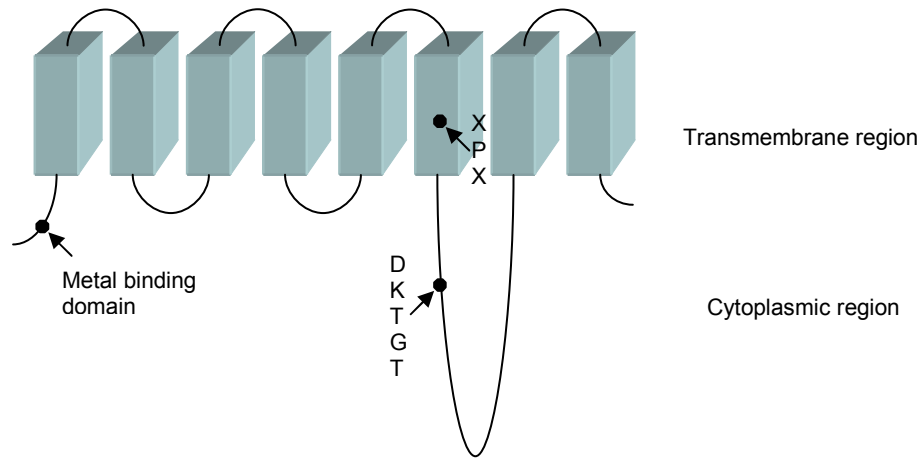
Fig. 2. General topology of P_{IB}-type ATPases. The transmembrane fragments are represented as grey boxes. The concensus sequence containing the phosphorylation site is indicated in the long cytoplasmic loop. xPx sequence in the sixth fragment and metal binding domain in N-terminus are also indicated.

It has been proposed that the side chains of the residues in the CPC in the sixth transmembrane fragment (TM6) would participate in the metal coordination and transport [9]. This has been supported by experimental evidence for some Cu-ATPases [80, 85]. However, this motif would not be sufficient for metal specificity, as proteins with the same xPx sequence in TM6 transport different metal ions. For instance, both the human ATP7B and the *E. coli* ZntA proteins contain CPC in TM6, but they transport Cu^+/Ag^+

and $Zn^{2+}/Cd^{2+}/Pb^{2+}$ respectively [78, 86]. To investigate metal specificity determinants in P_{IB}-ATPases, Argüello proposed a subdivision of these proteins based on signature sequences present in TM7 and TM8 [84]. These transmembrane fragments are structurally equivalent to the fragments TM5 and TM6 of the P_{II}-ATPases, which were shown to be responsible for ion binding during transport [74, 83, 87, 88]. By alignment of 234 P_{IB}-ATPases sequences, proteins were divided in groups IB-1 to 4 predicted to transport: Cu^+/Ag^+, $Zn^{2+}/Cd^{2+}/Pb^{2+}$, $Cu^{2+}/Cu^+/Ag^+$ or Co^{2+} respectively; while other proteins fell in two definite groups with non-predicted metal specifity (IB-5 and IB-6) [84].

The role of the N- or C- terminus metal binding domains (MBD) is not completely clear, but it has been postulated to be regulatory rather than required for ion transport [80, 82, 89-92]. In our laboratory, it has been shown that mutations in the C-MBD of CopA from *A. fulgidus*, had no effect on the enzymatic activity, phosphorylation, E_1-E_2 equilibrium or apparent binding affinities [80]. On the other hand, mutations in its N-MBD did not affect E_1-E_2 equilibrium, nor metal or ATP binding apparent affinities, but decreased the E_2.P dephosphorylation rate and therefore the enzyme turnover (~40%) [80]. Similar results were obtained in our laboratory for the Cu^{+2}-ATPase, CopB, from *A. fulgidus* [82]. Removing the N-MBD of CopB affected the enzyme activity by lowering the dephosphorylation rate [82]. Also in support of a regulatory role, isolated N-MBDs from Wilson's disease protein were shown to interact with the ATP binding domain in a Cu-dependant manner [89]. Finally, some P_{IB}-ATPases do not have any metal binding domain in the cytoplasmic regions, suggesting that MBDs are not essential for metal transport.

The relevance of P_{IB}-ATPases in metal homeostasis is well illustrated when analyzing the role of the human ones. Only two P_{IB}-ATPases have been identified in humans and both transport Cu^+ outwards from the cytoplasm. Defects in ATP7A protein lead to Menkes' disease while defects in ATP7B protein results in Wilson's disease. The former one is associated with Cu^+ deficiency in peripheral organs and central nervous system due to reduced transport of dietary Cu^+ across the basolateral membrane of enterocytes. Menkes' disease is usually lethal at an early age. On the other hand, Wilson's disease is characterized by intracellular accumulation of Cu^+ in liver, reduced

excretion through the bile and accumulation in other tissues, including brain. The different clinical effects observed in Menkes' and Wilson's diseases are explained by differences in tissue-specific expression of these proteins (ATP7A is predominantly expressed in enterocytes and endothelium of the blood barrier; ATP7B is mainly expressed in liver and to a lesser extent in brain, kidneys, placenta and heart) [86].

Here, we report studies on P_{IB}-ATPases from different organisms. The work is divided in two parts. The first one focuses in a group of ATPases from *Arabidopsis thaliana* plants. The second part describes a novel Pb-transport ATPase from a thermophilic archaeabacterium, *Aeropyrum pernix*.

PART I: PLANTS P$_{IB}$-ATPASES

P$_{IB}$-ATPases in *Arabidopsis thaliana*

Eight putative P$_{IB}$-ATPases (HMA1-8) have been identified in *A. thaliana* by sequence analysis. Four of them, HMA5-8, are predicted to transport Cu$^+$ and Ag$^+$; HMA2, 3 and 4 are proposed to be Zn^{2+}/Cd^{2+}/Pb^{2+}-ATPases; and HMA1 would be a Co^{2+}-ATPase [84]. The presence of Zn^{2+}-ATPases in *Arabidopsis* is particularly interesting since plants are the only eukaryotes with representatives from this group of proteins.

Experimental evidence of a role of HMA6 and HMA8 in Cu$^+$ transport was obtained by analyses of mutant plants [93, 94]. These plants exhibited a high chlorophyll fluorescence suggesting that the photosynthetic electron transport was defective. It was shown that in both mutants the Cu levels were normal in shoots but reduced in chloroplast, and that the phenotype could be rescued by adding external Cu. The presence of a functional chloroplast targeting sequence was also shown for HMA6 and HMA8 proteins. It has been suggested that HMA6 localizes to the envelope and HMA8 to the thylakoids. Altogether, these results suggested that HMA6 and 8 are implicated in Cu$^+$ transport from the cytosol into the chloroplast [93-95]. From sequence analysis [84], yeast complementation assays [96] and studies with mutant plants [96-98] HMA5 and HMA7 have been proposed to transport Cu$^+$. HMA5 was proposed to have a role in Cu detoxification in roots [98], while HMA7 is hypothesized to deliver Cu$^+$ to ETR1 (Cu dependant ethylene receptor) in post-Golgi vesicles [96, 97]. Two proteins from subgroup IB-2, HMA3 and HMA4, have been partially described. In mutant yeast cells, HMA3 expression rescued the Cd^{2+}/Pb^{2+}-hypersensitivity phenotype. In addition, the Cd^{2+} levels in wild type and HMA3-expressing cells were similar. With this, a role in intracellular Cd^{2+} sequestration was proposed for HMA3 [99]. A similar approach was used to analyze HMA4, where complementation assays performed with mutant bacteria and yeast cells suggested a role of this ATPase in Zn^{2+} and Cd^{2+} transport [100]. For HMA3 and HMA4 transcription levels in various organs were analyzed by RT-PCR showing different patterns for these genes [99, 100]. HMA3-GFP fusions were observed at vacuoles [99] suggesting a role in Cd/Pb detoxification. HMA4 tissue localization was analyzed by

fusion with a reporter gene, and shown to be expressed in vascular tissue of roots, stems and leaves[101]. In our laboratory, characterization of HMA2 has been done [102]. ATPase activity was stimulated by Zn^{2+} and Cd^{2+} and to a lesser extent by other divalent metal ions. Phosphorylation of the enzyme and characteristic inhibition by vanadate were also shown. The direction of the transport was determined in yeast vesicles expressing HMA2, suggesting a role of this protein in the efflux of Zn^{2+} from the cytosol. This was supported by the observation of Zn^{2+} accumulation in *hma2* mutant plants. This publication represents the first work where transport and activity assays were performed. Furthermore, this represents the first experimental evidence for a Zn^{2+}-ATPase in eukaryotes.

Goals of this study

As it was mentioned above, *Arabidopsis thaliana* has eight genes encoding P_{IB}-ATPases. This number is strikingly high when compared, for instance, with human P_{IB}-ATPases. In addition, the plant transporters present more variety of substrates as there are representatives of subgroups IB-1, 2 and 4 [84]. The questions that arise then are: why does *Arabidopsis* have such a large number of heavy metal ATPases and why does it have more than one that seems to transport the same metal ions (i.e. HMA2-4 and HMA5-HMA8)? One possible answer to these questions is that different P_{IB}-ATPases are expressed in different parts of the plants and/or the cells, having distinctive functions according to their localization. In this direction, this part of the work was focused on the functional characterization of three of these proteins: HMA3, HMA4 and HMA8. To accomplish this aim, individual goals were proposed:

- Determine metal specificity and biochemical parameters by expressing the proteins in heterologous systems and determining ATPase activity in the presence of different metals.
- Check for transcript levels of the genes in different organs and in plants exposed to various metals by semiquantitative RT-PCR analysis and using reporter genes.
- Analyze the effects of removing the genes from *Arabidopsis*.

RESULTS

Bioinformatic analysis

The gene, cDNA, and protein sequences of HMA3, HMA4 and HMA8 were obtained from a database (http://www.ncbi.nlm.nih.gov/entrez/query.fcgi). The gene coding for *HMA3* (At4g30120) is 3102 bp long, the resulting mRNA is 2283 bp long distributed in 9 exons (Fig. 3). The protein length is 760 aminoacids and its molecular weight is 81,950 Da. *HMA4* gene (At2g19120) is 6778 bp long and encodes for a 9 exons mRNA of 3519 bp long (Fig. 3). The protein length is 1172 aminoacids and its molecular weight is 127,208 Da. *HMA8* gene (At5g21930) is 5593 bp long and encodes for a 2571 bp long mRNA of 17 exons (Fig. 3). The protein length is 856 aminoacids and its molecular weight is 90,843.2 Da.

The general exon-intron distribution for HMA3 and HMA4 is similar, i.e. equal number of exons, relatively long exon 9 and most of the introns are short compared with exons length. The main difference between these two genes maps is the length of introns 1 and 2. It has been proposed that this similarity could have resulted from ancestral gene duplication with subsequent additions or deletions [103]. On the other hand, the number of exons in HMA8 gene is larger and most of them are shorter than 100 bp (Fig. 3).

Fig. 3 Exons-Introns map. Schematic representation of exons (black boxes) and introns (gray boxes) for At4g30120 (*HMA3*), At2g19120 (*HMA4*) and At5g21930 (*HMA8*) genes.

A series of web-based prediction software is available to analyze putative topology of membrane proteins, subcellular localization, secondary-tertiary structures, etc. (http://au.expasy.org/). Here, we used two of these tools to predict the topology of HMA3, HMA4 and HMA8 proteins: TMHMM (http://www.cbs.dtu.dk/services/TMHMM-2.0) and TMpred (http://www.ch.embnet.org/software/TMPRED_form.html). The three proteins were predicted to have eight transmembrane fragments. Both HMA3 and HMA4 have a relatively short N-terminus with no metal binding domains in them. While their C-terminus is long compared to HMA8 and contain putative metal binding domains (CCSGCC for HMA3, 11 histidines stretch for HMA4). On the other hand, HMA8's N-terminus is longer and has a CGGC sequence.

As mentioned before, Argüello [84] has subdivided the P_{IB}-ATPases according to the proposed transported metal based on consensus sequences in the transmembrane fragments 7 and 8 (TM7 and TM8). These conserved residues contain side chain atoms with ability to coordinate metals. Therefore, they are hypothesized to determine the metal-specificity. Fig. 4 shows the sequence alignment of these fragments from HMA3 and HMA4 with representatives of $Zn^{2+}/Cd^{2+}/Pb^{2+}$-ATPases and HMA8 with Cu^{+}/Ag^{+}-ATPases. $Zn^{2+}/Cd^{2+}/Pb^{2+}$-ATPases possess the signature sequence $NX_7KX_{10-20}DXGX_7N$; while in Cu^{+}/Ag^{+}-ATPases the conserved sequence in TM7 and TM8 is $NX_6YNX_4PX_{5-25}PX_6MX_2SSX_6S$.
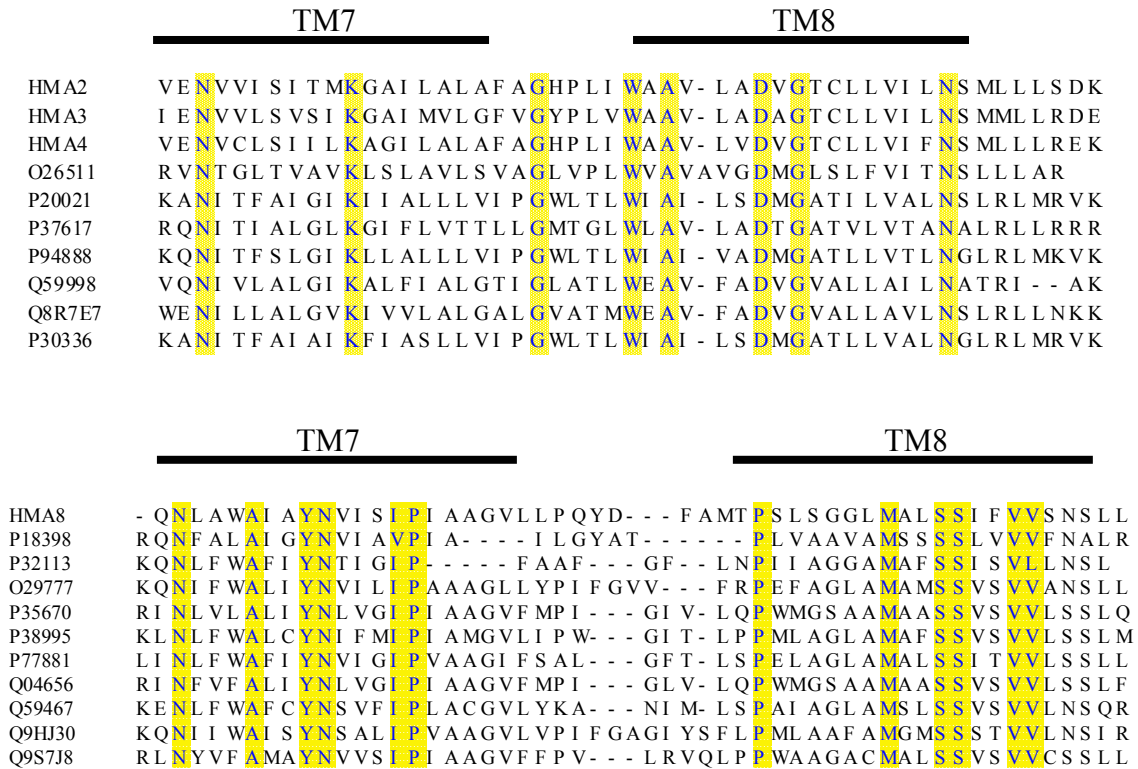
Fig. 4. Alignment of the TM7 and TM8 of HMA3, HMA4 and HMA8 with other Zn^{2+}/Cd^{2+}/Pb^{2+}- or Cu^{+}/Ag^{+}-ATPases. Protein accession numbers are shown in the left column. Horizontal bars indicate the spanning of TM7 and TM8. Vertical bars highlight conserved residues with potential metal coordinating side chains.

Isolation of cDNAs and cloning in bacteria and yeast expression vectors

In order to start the experimental analysis of HMA4 and HMA8, the cDNAs coding for these proteins were cloned in bacteria and yeast expression vectors. HMA4 cDNA had been previously cloned in a bacterial expression vector (pBAD-TOPO) in our laboratory.

To clone HMA8, total RNA was extracted from 4-weeks-old leaves, first strand cDNA was obtained by reverse transcription and the cDNA was amplified by PCR with specific primers (Fig. 5A). In this amplification, restriction sites (KpnI and XhoI) were added at both sides of the sequence for further cloning in yeast expression system. HMA8 cDNA was purified, ligated to pBAD-TOPO vector and TOP-10 *E. coli* cells were transformed. The right size and orientation of the insert was checked by restriction digestion (Fig 5B). To verify the absence of mutations that could have occurred during

the PCR as well as, the absence of shifts in the open reading frame HMA8 cDNA was fully sequenced using specific primers annealing to the sequence every 400 bp.

HMA4 and HMA8 cDNAs were released by restriction digestion from the HMAs-pBAD-TOPO constructs and subcloned in pYES2/CT vector at KpnI/EcoRI and KpnI/XhoI sites respectively. These constructs were initially introduced in TOP-10 *E. coli* cells and checked for right orientation by PCR and restriction digestion (Fig 5C and 5D). For this PCR screening, short fragments of the cDNA were amplified (about 1.5 kb and 1.3 kb for HMA4 and HMA8 respectively). Digestion of HMA4-pYES2/CT with HindIII enzyme yielded two fragments of 3 kb and 6.4 kb, while digestion of HMA8-pYES2/CT with SpeI yielded fragments of 1.3 kb and 7.2 kb, as expected. Yeast cells were transformed with the constructs by electroporation and transformants were selected in media without uracil.
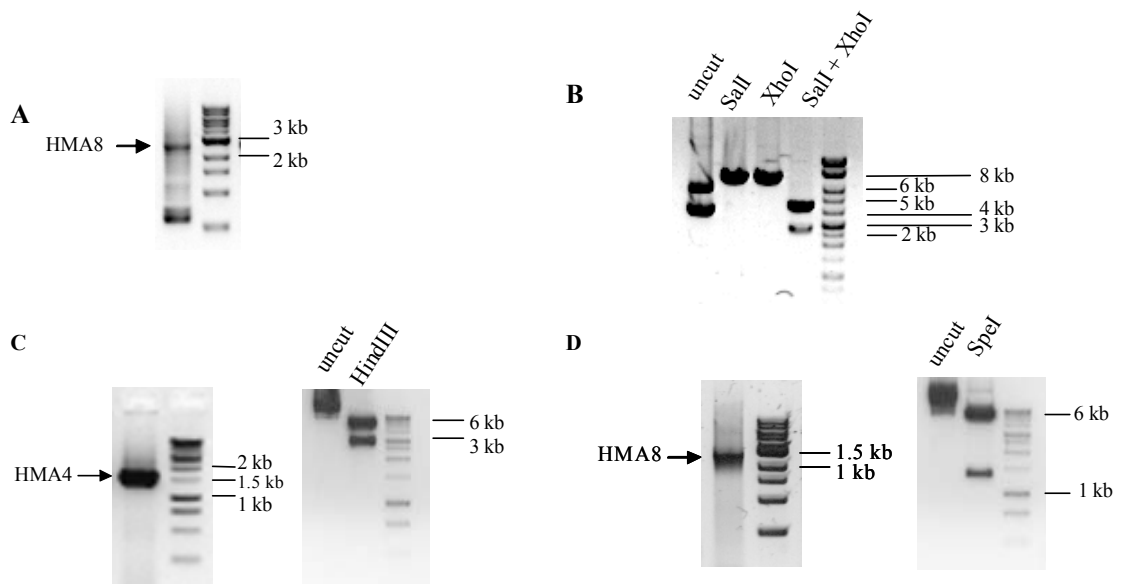
Fig. 5. Cloning of HMA4 and HMA8. HMA8 cDNA (~2.5 kb) was amplified by RT-PCR from leaves (**A**). Restriction digestion of HMA8-pBAD-TOPO (**B**). HMA4 and HMA8 were subcloned in pYES2/CT vector, PCR screening and restriction digestion are shown (**C** and **D** respectively). 1% agarose gels stained with ethidium bromide are shown.

Expression in heterologous systems

Expression assays were performed in TOP10 *E. coli* cells carrying the HMA8-pBAD-TOPO contruct. This vector has an arabinose-inducible promoter and a polyhistidine (6xHis) tag in the 3' of the cloning site for immunodetection and purification. The expression was induced for 2 and 4 hours by adding different concentrations of arabinose at room temperature or at 37°C. The presence of HMA8 protein (~90kDa) was checked by western blot using an antibody against the His-tag. No expression was detected in any case (not shown). HMA3 and HMA4 expression in bacteria had been previously checked in the lab with similar results. So, expression of these proteins was attempted in yeast. Both HMA4 and HMA8 were successfully expressed in this system (Fig. 6). A single band was detected for HMA8 protein, while for HMA4 extra bands of lower size were observed. These could be HMA4 degradation products. Membrane enriched fractions were prepared for both proteins. ATPase activity was measured in these fractions, but no activities over the background could be detected (not shown). This result could be explained by the low levels of expression of each protein and the high number of other ATPases present in yeast membranes. Attempts to purify the proteins were unsuccessful (not shown).
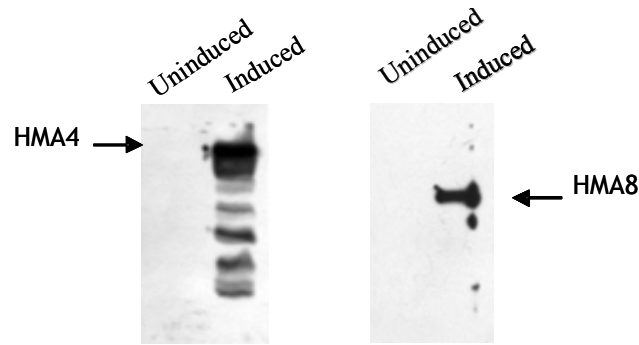
Fig. 6. Expression of HMA4 and HMA8. HMA4 and HMA8 were expressed in yeast cells. Protein lysates from Uninduced or Induced cells were separated in 10% SDS-PAGE, immunostained with AntiHis antibody. The bands corresponding to HMA4 or HMA8 are indicated by an arrow.

Organ specific expression

The presence in the plants of several proteins transporting the same metal ions could be explained by different functions *in planta*. This could be a result of distinct expression patterns at the tissue or subcellular level. Other possible explanation could be that the transporters are differentially regulated, i.e. their expression varies upon diverse stimuli. To investigate the expression pattern of the genes in the plant tissues, semiquantitative RT-PCR was performed using total RNA from seedlings, roots, stems, leaves and flowers.

The pattern observed for the three genes was different among them and from other Zn^{2+}-ATPases and Cu^{+}-ATPases analyzed in our lab, supporting the starting hypothesis of differential expression in the plant. HMA3 transcript was detected only in seedlings, while HMA4 was detected mainly in roots and to a lesser extent in seedlings, leaves, stems and flowers (Fig. 7). HMA8 was detected in all the tested organs, with higher transcript levels in seedlings and leaves (Fig. 7). Similar results were obtained for HMA8 when the expression pattern was analyzed by northern blot (not shown).
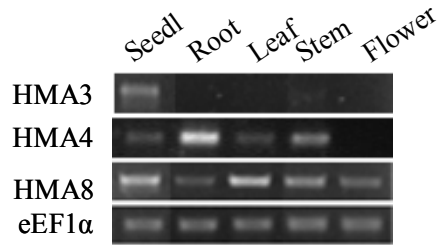
Fig. 7. HMA3, HMA4 and HMA8 organ specific expression. Semiquantitative RT-PCR was used to determine transcript levels of HMA3, HMA4, HMA8 or the transcription factor eEF1α in the indicated organs of 6-weeks-old plants. 1% agarose gels stained with ethidium bromide are shown.

To further investigate specific expression of HMA8 protein, the promoter of its gene was cloned upstream the reporter gene β-glucurodinase (GUS) in the vector pDESTG2. pDESTG2 is a GUS expression vector adapted to the Gateway cloning technology. This system uses bacteriophage lambda-based site-specific recombination instead of cloning with restriction enzymes and ligase. Genes are first cloned into the "entry vector" and then subcloned (by recombination) into the "destination vector".

In this work, a stretch of 2050 bp upstream the start codon of HMA8 mRNA was amplified by PCR using the BAC T6G21 as a template (Fig. 8A). HMA8 promoter region was first cloned in the entry vector pENTR-D/TOPO. TOP10 *E. coli* cells were transformed and checked for the construct by PCR and restriction digestion with BsrGI enzyme that cuts at both sides of the insert (Fig. 8B). Then, the promoter was subcloned into pDESTG2 by recombination reaction, TOP10 *E. coli* cells transformed and the construct analyzed by PCR screening and restriction digestion with the BsrGI enzyme (Fig. 8C). Finally, *Agrobacterium tumefaciens* cells (GV2260) were transformed with the construct by electroporation and the colonies were screened by PCR to check for the presence of the promoter sequence (Fig. 8D).
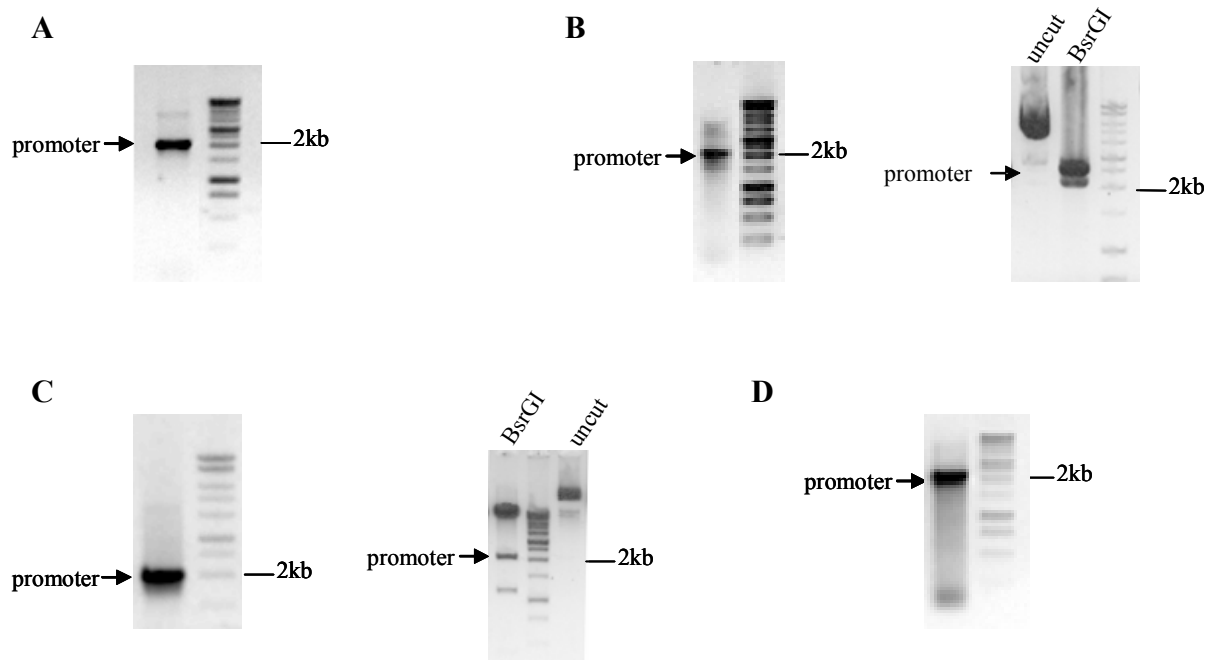
Fig. 8. Cloning of HMA8 promoter in pDESTG2 vector. HMA8 promoter was amplified (2050 bp) by PCR (**A**). PCR screening and restriction digestion of promoter in pENTR-TOPO (**B**) and pDESTG2 (**C**) vectors. PCR screening of promoter-pDESTG2 in Agrobactrium tumefaciens (**D**)

Arabidopsis thaliana plants were transformed with *Agrobacterium tumefaciens* holding the construct HMA8-promoter-pDESTG2 by floral dip as described in Experimental Procedures. Two transgenic plants were identified in agar selective plates, transplanted to soil, grown and checked for β-glucurodinase activity. As shown in Fig. 9, both transgenic lines showed GUS activity in leaves, cauline leaves and flowers. These results are in agreement with the pattern observed in RT-PCR studies (Fig. 7).

Fig 9. GUS staining of transgenic plants. Leaves (upper panel) and cauline leaves (middle panel) from plants untransformed (left) or two HMA8-promoter-pDESTG2 transgenic lines (middle and right) are shown. A 20X magnification of a flower from a transgenic line is shown (bottom panel).

Expression regulation by metals

As all the mRNAs were detected in seedlings, we further tested the effects of exposing seedlings to different metals. In order to do this, seeds were plated in media in the absence of metals (control) or in the presence 0.1 mM $CuSO_4$, 0.5 mM $ZnSO_4$, 0.25 mM $CdCl_2$, 0.25 mM $NiSO_4$, 0.25 mM $CoCl_2$, 0.1 mM $AgNO_3$ or 0.5 mM $MnCl_2$. Total RNA was extracted from seedlings and RT-PCR was performed. HMA3 transcription was induced upon treatment with Ag^+, Co^{+2} and Mn^{+2}; HMA4 levels were increased by Zn^{+2}, Cd^{+2} and Ni^{+2}; and HMA8 transcription was up-regulated in seedlings grown in Cu^{+2}-containing media (Fig. 10). The effects observed for HMA8 and HMA4 are in accordance with the metal selectivity proposed for these two ATPases (Cu^+/Ag^+ and $Zn^{2+}/Cd^{2+}/Pb^{2+}$ respectively). However, it should be noticed that from this kind of

17

experiments no conclusions about metal specificity can be drawn. To further demonstrate metal specificity of these proteins biochemical determinations should be carried out.
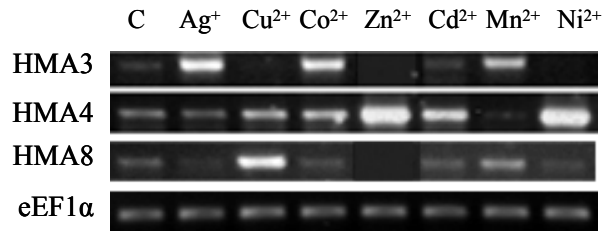
Fig 10. Expression regulation by metals. Semiquantitative RT-PCR was used to determine transcript levels of HMA3, HMA4, HMA8 or the transcription factor eEF1α in seedlings grown in plates with no metal (C); 0.1 mM Ag^+; 0.1 mM Cu^{2+}; 0.25 mM Co^{2+}; 0.5 mM Zn^{2+}; 0.25 mM Cd^{2+}; 0.5 mM Mn^{2+} or 0.25 mM Ni^{2+}.

Screening of mutant plants

One approach to study protein function in an organism is to remove its gene expression (also called, knock-out). In order to do this, seeds containing ~4.3 kb T-DNA insertions (T_3 generation) in the P_{IB}-ATPases genes under study were obtained from the *Arabidopsis* Biological Resource Center (ABRC).

Seeds from line SALK_050924, with an insertion in the exon 4 of At2g19110 gene (*HMA4*) or line SALK_037789 containing an insertion in the exon 8 of At5g21930 gene (*HMA8*) were studied. Seeds were grown in soil and homozygous plants for the insertion were identified by PCR screening using genomic DNA as a template (Fig. 11). Seeds (T_4 generation) were obtained from these homozygous plants. The seeds were grown in soil for 4 weeks, total RNA was obtained and semiquantitative RT-PCR was performed using primers encompassing the region of the T-DNA insertion to confirm the absence of HMA4 or HMA8 transcripts (Fig. 11).

18
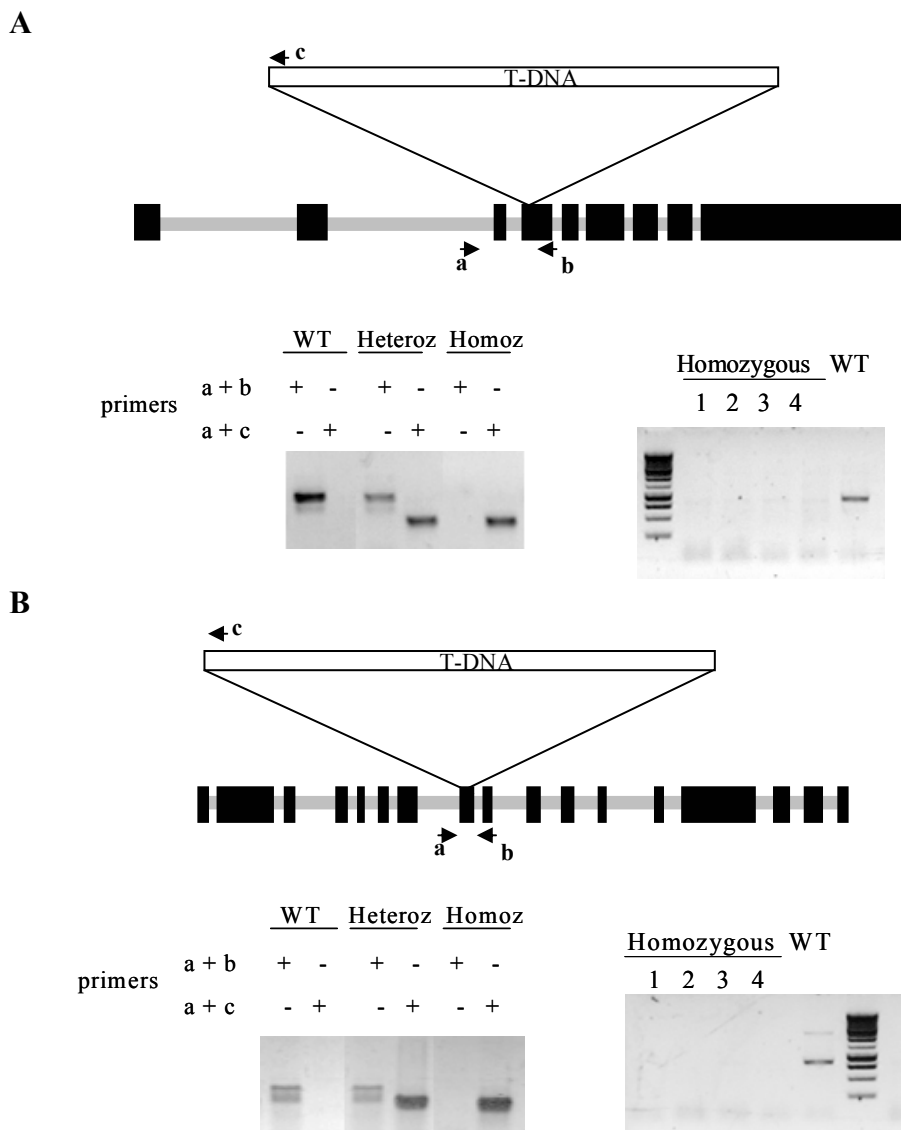
Fig. 11. Exon-intron map and PCR screening of SALK lines. Upper panels show the localization of the T-DNA insertion in the exon-intron map for *HMA4* gene in the line SALK_050924 (**A**) and *HMA8* gene in the line SALK_037789 (**B**). The annealing position of the primers (**a**, **b**, **c**) used for PCR screening is also indicated. In bottom panels left, 1% agarose gel stained with ethidium bromide shows PCR screening for WT, heterozygous and homozygous plants. The pair of primers used in each lane is indicated. In right bottom panels, RT-PCR from knock-out and WT plants (1 to 4 represent four different plants from same line) using primers for HMA4 or HMA8.

Mutant plants for both HMA4 and HMA8 showed a similar macroscopic morphology to wild type plants when grown in soil under normal conditions (i.e. no metal additions or other treatment) (not shown). Further studies should be performed to determine how the absence of these genes affects the plants under different treatments and at a microscopic level.

PART II: PbtP: a novel lead-ATPase from *A. pernix*

As mentioned in the Introduction section, typically, most P_{IB}-ATPases have eight transmembrane segments (TMs), one or more metal binding domains in the cytoplasmic N-terminal region and a series of amino acids conserved in all the members of this family. By sequence homology analysis of the last three TMs of P_{IB}-ATPases, the metal specificity for most of these enzymes has been predicted [84]. Here we report a thermophilic P_{IB}-ATPase from *Aeropyrum pernix* with a novel metal specificity. Our laboratory has been very successful with the characterization of other thermophilic ATPases [80-82]. We have named the protein under study as PbTP (gene APE2571). The interest in this enzyme arises from its particular structural features, as it is smaller than other P_{IB}-ATPases, it is predicted to have only six transmembrane segments and no metal binding domains in N- or C-termini as represented in Fig. 12.
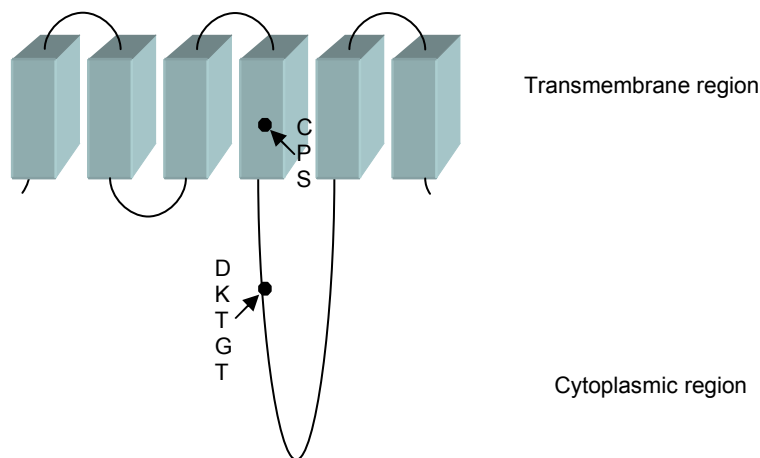
Fig. 12. Predicted topology of PbTP. The transmembrane fragments are represented as grey boxes. The consensus sequence containing the phosphorylation site is indicated in the long cytoplasmic loop. CPS sequence in the sixth fragment is also indicated.

Another peculiarity of this enzyme is that when comparing PbTP amino acid sequence with other reported ATPases, no metal selectivity can be assigned because it lacks the characteristic conserved residues responsible for metal selectivity in the last TMs [84]. As an example, the partial alignment of nine Zn/Cd/Pb-ATPases from different

organisms together with PbTP is shown in Fig. 13. Only a few consensus amino acids in the Zn/Cd/Pb-ATPases subgroup are present in TMs 5 and 6 of PbTP (compare with Fig. 4). Interestingly, two Asn residues (indicated with red dots in Fig. 13) which have been shown to be critical for activity of a Cu-ATPase [104], are replaced by a Gly and Ala in TM7 and TM8 respectively. Another peculiarity of PbTP is the presence of a CPS sequence in TM6. Altogether, it suggests that PbTP has an unusual metal specificity.
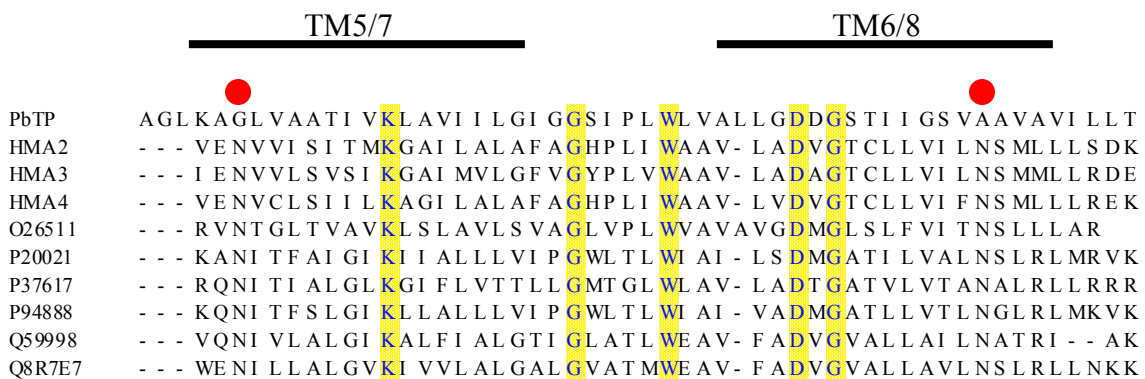
Fig. 13. Alignment of the TMs 7 and 8 of Zn^{2+}/Cd^{2+}/Pb^{2+}-ATPases and TMs 5 and 6 of PbTP. Protein accession numbers are shown in the left column. Horizontal bars indicate the spanning of TM5 or 7 and TM6 or 8. Vertical bars highlight conserved residues with potential metal coordinating side chains. ● Indicates non conserved residues in PbTP.

Goals of this study

The aim of this part of the work was to characterize PbTP. Identifying the metal selectivity and catalytic activity of this small representative of P_{IB}-ATPases could shed light on the general mechanism of this family of proteins. In this direction, individual goals were proposed:

- Express PbTP in *E. coli.*
- Determine metal specificity and biochemical parameters by measuring ATPase activity in the presence of different metals.

22

RESULTS

PbTP expression and purification

In order to characterize this enzyme, the cDNA coding sequence was cloned into the bacterial expression vector pBAD-TOPO. The 67kDa protein was expressed in *Escherichia coli* as described in the Experimental procedures section. Fig. 14A shows a SDS-PAGE stained with Coomassie brilliant blue and the immunodetection of PbTP using a specific antibody against the His-tag. PbTP was partially purified in an affinity column (Fig. 14B).
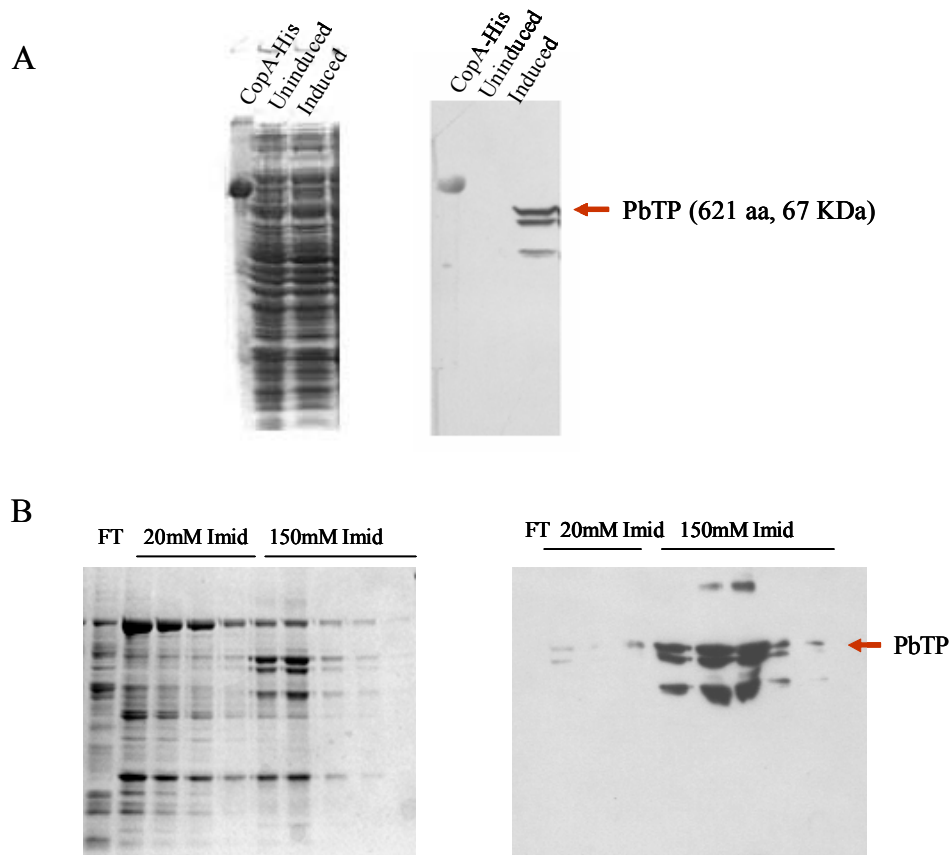
Fig. 14. PbTP expression and purification. PbTP was expressed in E. coli and partially purified by affinity chromatography. Protein lysates from Uninduced or Induced cells were separated in 10% SDS-PAGE, stained by Coomassie blue (**A**, left) or immunostained with AntiHis antibody (**A**, right). The band corresponding to PbTP is indicated by an arrow. CopA-His protein was used as a positive control for immunostaining. Proteins from purification fractions were separated and stained as before (**B**). Fractions: flow through (FT), washes 1 to 4 with 20mM imidazole and elutions 2-6 with 150mM imidazole are shown (**B**).

Both the levels of expression and purification were low. In order to improve them, subcloning into different expression vectors was performed and expression was attempted. No expression was obtained in any case (data not shown).

Metal dependent ATPase activity

To determine the metal specificity of PbTP, the ATP hydrolysis by the enzyme was determined in the presence of various metals (Fig. 15). Interestingly, the enzyme retained its thermophilicity characteristics when isolated from its native lipid environment. The metal dependent ATPase activity was determined at 75ºC. The enzyme was highly activated by Pb^{2+} (Vmax: 23.6 µmol Pi/mg/h) and to a lesser extent by Zn^{2+}, Hg^{2+} and Cd^{2+}. Another interesting feature is the activation by Hg^{2+}, to date no P_{IB}-ATPase has been reported to transport this metal ion.
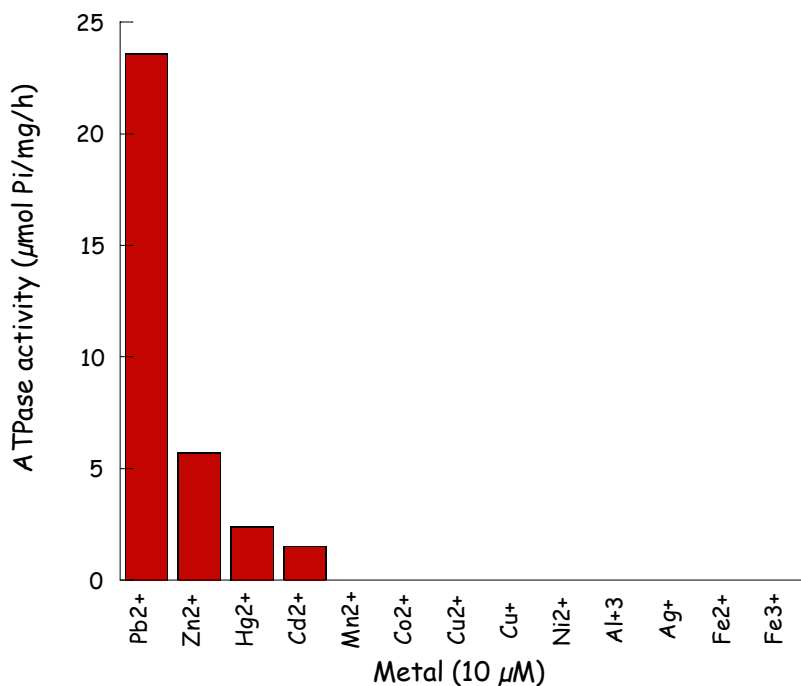
Fig. 15. Activation of PbTP ATPase activity by different metals. ATP hydrolysis was determined at 75˚C using partially purified protein in the presence of the indicated metals (10µM).

24

The ATPase activity was also measured in membrane enriched fractions, in the presence of different concentrations of Pb^{2+} (Fig. 16). Lead was shown to interact with PbTP with high apparent affinity ($K_{1/2}$: 4.6 µM).
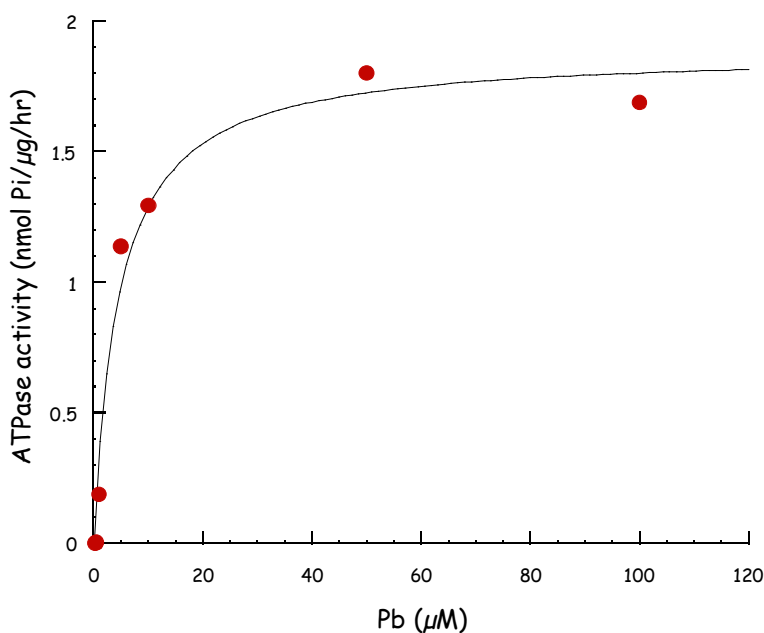
Fig. 16. Pb^{2+} dependent-ATPase activity. ATP hydrolysis was determined at 75˚C using membrane enriched fractions in the presence of the indicated Pb^{2+} concentrations.

It has been previously shown that milimolar levels of thiolates such as cysteine or gluthatione can activate some heavy metal ATPases [79, 81]. In order to determine if a similar effect occurs with PbTP, the Pb^{2+}-stimulated ATPase activity was measured in the presence of 20 mM cysteine (data not shown). The enzymatic ATP hydrolysis was independent of cysteine, suggesting direct interaction of the metal ions with the transmembrane transport sites.

DISCUSSION

Plant heavy metal transport ATPases

The presence of numerous members of the P_{IB}-ATPases family in *Arabidopsis thaliana* makes it a very interesting system of study. Identifying the physiological role of each of these proteins can provide information about evolution of these proteins in plants as well as tools for future applications such as bioremediation. In this work we presented evidence of distinct expression patterns and regulation by metals for HMA3, 4 and 8 by RT-PCR (Fig. 7). Based on different localization, yeast complementation assays and phenotypes in mutant plants, it has been proposed that HMA2 and HMA4 participate in Zn transport from roots to shoots, HMA7 and HMA8 in Cu delivery to metallochaperones and HMA5 in Cu detoxification in roots [93, 102, 105, 106].

HMA4 transcription was observed mainly in roots and to a lesser extent in seedlings, leaves and stems while HMA3 was only detected in early stages of development. Using the same approach, other authors reported a similar pattern for HMA4 [107] [99]. Interestingly, the same research group reported later that HMA4 expression was higher in flowers than other organs and HMA3 could be detected in leaves and roots [105]. A plausible explanation for these contradictory results would be that they studied HMA4 in two different *A. thaliana* ecotypes (Col-0 and Ws respectively) and HMA3 from Ws ecotype. Distinct effects were observed on both Zn-ATPases levels when the seedlings were grown in the presence of metals (Fig. 10) while for HMA2 little or not effect was reported [102].

HMA8 expression was detected in all the analyzed organs. These results were confirmed by northern blot (not shown) and by the GUS expression pattern observed in transgenic plants (Fig. 9). Recently, HMA8 transcription was reported to occur in shoots but not roots [93]. In agreement with other Cu-ATPases [98], we observed increased transcription levels of HMA8 in seedlings exposed to copper.

Finally, there is also evidence for different subcellular and tissue localization for some of the P_{IB}-ATPases in *A. thaliana* [93, 101, 105]

Altogether, these results support the starting hypothesis of different roles *in planta* determined by the specific spatial and/or temporal distribution. Similarly, the two human Cu-ATPases differ in tissue-specific expression and therefore they show different functions [86].

To date, actual metal specificity and transport has been shown only for HMA2 in our laboratory [102], in this direction protein expression in heterologous systems is the first step towards the biochemical characterization of these enzymes. Here we obtained expression of HMA4 and HMA8 in yeast cells. So far, our attempts to measure enzymatic activity were unsuccessful. This is not surprising if we consider the large number of research groups who are working with eukarytic P_{IB}-ATPases and the lack of reports on biochemical characterization. Further efforts will be performed to study these proteins.

.

Archaeal heavy metal transport ATPases

Studies on enzymes from extremophilic organisms can provide insight into determinants of protein thermostability. *Aeropyrum pernix* is an aerobic hyper-thermophilic archaeon. It has been isolated from a thermal vent located in an island off of Japan where it grows at temperatures around 90ºC. PbTP shows particular features when compared to other P_{IB}-ATPases: it is a small protein with only six predicted transmembrane fragments, it has a CPS sequence in its fourth TM, it shows no cytosolic metal binding domains and its metal specificity could not be predicted by sequence analysis [84].

In the present work, we cloned the coding sequence for PbTP into a prokaryotic system, expressed and partially purified the functional protein (Figs. 14-16). Although the lipid environment was changed (archaeon vs prokaryote), the enzyme conserved its thermophilicity as it showed ATPase activity at 75ºC. The highest PbTP ATPase activity was observed in the presence of Pb^{2+} (Vmax: 23.6 µmol Pi/mg/h). Lower levels of activity were measured in the presence of other divalent ions ($Zn^{2+}>Hg^{2+}>Cd^{2+}$). Comparable values have been reported for Pb^{2+}, Zn^{2+} and Cd^{2+} for the *E. coli* Zn-ATPase, ZntA [108].

In vivo, metal ions delivery to ATPases may be mediated by metallochaperones. The chaperone role *in vitro* can be simulated by addition of thiolates in the reaction

media. It has been shown that other studied P_{IB}-ATPases require thiolates such as cysteine or gluthathione to be fully active [81] [108]. In our case, PbTP did not show changes in activity upon incubation with cysteine suggesting that the metal ions interact directly with the transport site.

To our knowledge this is the first Pb^{2+}-ATPase reported in archaebacteria, and the first Hg^{2+}-activated ATPase.

EXPERIMENTAL PROCEDURES

Plant Growth

Arabidopsis thaliana (Ecotype Col-0) and T-DNA insertional mutant plants seeds were surface sterilized for 1 min in 70% (v/v) ethanol followed by soaking for 5 min in 1.25% (v/v) bleach solution supplemented with 0.02% (v/v) Triton-X100. Vernalization was induced by keeping the seeds at 4°C for 48 h before placing them in a plant growth chamber at 22°C, 10,000-14,000 lux cool-white fluorescent light intensity under a cycle of 14/10 h day/night. Seedlings were grown vertically on 2% agar, Murashige and Skoog salt mixture with vitamins (GIBCO BRL, MD) supplemented with one of the following metals: 0.5 mM $ZnSO_4$; 0.5 mM $MnCl_2$; 0.25 mM $CdCl_2$; 0.25 mM $NiSO_4$; 0.25 mM $CoCl_2$; 0.1 mM $CuSO_4$; 0.1 mM $AgNO_3$ or no metal (control). Seedlings were collected 13-15 days after germination. Leaves, roots, stems and flowers were harvested from 6 weeks-old plants. For experiments with T-DNA insertion lines, leaves were harvested after 2 or 3 weeks of growth for genomic DNA (gDNA) extraction or after 4 weeks for RNA extraction.

HMA8 cloning

Total RNA was obtained from 100 mg of 4-weeks-old leaves using the RNAeasy Plant Mini kit (QIAGEN Inc, Valencia, CA) according to the manufacturer's specifications. The RNA integrity was verified with formaldehyde agarose gels [109]. First-strand cDNA was synthesized with Superscript II reverse transcriptase (Invitrogen, Carlsbad, CA) using oligodT$_{(18)}$ primer and 2 μg total RNA. Second strand synthesis was performed by polymerase chain reaction (PCR) using the first strand cDNAs as template and forward and reverse primers corresponding to 5' and 3' ends of HMA8 predicted coding sequence (http://www.ncbi.nlm.nih.gov/entrez; Gene Bank Accession #: AL589883). Forward primer: 5'-CCGGGTACCCCAATAATGGCGAGCAATCTTCTC-3'; Reverse primer: 5'-GGCTCGAGCAAGCTATTTTTACTTGTTTCAG-3'. Using these primers, the stop codon was removed, XhoI and KpnI restriction sites were added in 5' and 3' ends respectively and a yeast concensus sequence (AATA) was added upstream the initiation codon for further cloning into yeast expression vector. The PCR conditions were: 94°C 2 min; 15 cycles of 94°C 15 sec, 47°C 30 sec, 68°C 4 min followed by 25

cycles of 94°C 15 sec, 47°C 30 sec, 68°C 4 min + 20 sec/cycle. The resulting cDNA was purified and cloned into pBAD-TOPO vector (Invitrogen, Carlsbad, CA).

HMA8 cDNA was then sub-cloned into XhoI and KpnI sites of pYES2/CT vector (Invitrogen, Carlsbad, CA). This vector has a GAL1 promoter inducible with galactose, for high level protein expression in *Saccharomyces cerevisiae*; C-terminal peptide encoding for a polyhistidine tag (His₆) for detection and purification of the expressed fusion protein and URA3 auxotrophic marker for selection in yeast.

HMA3 and HMA4 cloning

HMA3 and HMA4 cDNAs had been previously cloned into pBAD-TOPO in our laboratory. Posterior sub-cloning into pYES2/CT vector was done using KpnI/EcoRI sites for HMA4. This construct was verified by PCR screening.

Cloning of HMA8 promoter into pDESTG2 vector

A stretch of 2050 bp upstream the start codon of HMA8 mRNA was amplified by PCR using the BAC T6G21 (kindly provided by the *Arabidopsis* Biological Resource Center) as a template and specific primers (Forward: 5'-CACCTGCTTGTCATCCTCATCCTTCTTGTT-3'; Reverse: 5'-GGCGAGACAGACGACGATAGTCAC-3'). The PCR conditions were: 94°C 2 min; and 30 cycles of 94°C 1 min, 50°C 1 min, 68°C 4 min. HMA8 promoter region was first cloned in the entry vector pENTR-D/TOPO (Invitrogen, Carlsbad, CA) and then into pDESTG2 by recombination reaction following the manufacturer's directions (Invitrogen, Carlsbad, CA). pDESTG2 vector was kindly provided by Dr. Elsbeth Walker (University of Massachussets, Amherst, MA.). Competent *Agrobacterium tumefaciens* cells (GV2260) were transformed with 100-500 ng DNA by electroporation (http://www-yeastlab.vbiol.slu.se/WCN/elporAgro).

Yeast transformation and expression of HMA4 and HMA8

Yeast strain INVSc1 (genotype: MATα his3Δ1 leu2 trp1-289 ura3-52; Invitrogen, Carlsbad, CA) was transformed with HMA4- and HMA8-pYES2/CT constructs by electroporation. The transformants were selected in uracil depleted SD media (6.7 g.l^{-1} yeast nitrogen base, 1.92 g.l^{-1} yeast synthetic drop-out media without uracil (Sigma) supplemented with 20 g.l^{-1} glucose). For expression assays, the cells were grown overnight at 30°C in SD medium without uracil and the expression was induced by addition of 2% galactose. Different expression times were studied. Protein concentration was estimated by Bradford method [110]; equal amounts were loaded in 10% polyacrylamide gels and separated by electrophoresis [111]. The gels were stained with Coomasie Brilliant Blue or blotted onto nitrocellulose for immunostaining with Anti-His antibody as the primary antibody (Santa Cruz Biotechnology) and horseradish peroxidase conjugated antibody as the secondary one (Affinity Bioreagents, CO).

Screening of T-DNA insertion lines

Seeds carrying a 4393 bp T-DNA insertion in exon 4 of the *HMA4* gene or in exon 8 of the *HMA8* gene (lines SALK_050924 and SALK_037789 respectively) were obtained from *Arabidopsis* Biological Resource Center (ABRC, Ohio). Genomic DNA was extracted from one leaf of 2-3 weeks-old plant [112]. Briefly, a leaf disc was macerated with plastic grinders (Scienceware, NJ) and 400 μl of extraction buffer were added (200 mM Tris-HCl pH 7.5, 25 mM EDTA, 250 mM NaCl, 0.5 % SDS). This homogenate was centrifuged for 1 min at 13000 rpm in a bench microcentrifuge, 300 μl of isopropanol were added to 300 μl of the supernatant, left for 2 min at room temperature and spun down for 5 min at 13000 rpm. The pellet was air-dried and resuspended in 40 μl of TE buffer. 2 μl of this solution were used for PCR screening.

Homozygous and heterozygous plants for the insertion were identified by PCR screening using two combinations of primers: a+b or a+c (schematic location of these primers is shown in Fig. 11). Primers sequences **a:** 5'-CCATACAAAGTCATGTGAATCCAA-3' and **b:** 5'-TGGTTATGTCTTTGCTTACCTGGA-3' for line SALK_050924; and **a:** 5'-TGTGGGTTTCCGAAAAGAGTTATGA-3'; **b:** 5'- CAGCTATTGCATCTGCCAGCC-

31

3' for SALK_037789 line; **c:** 5'-GCGTGGACCGCTTGCTGCAACT-3' for both lines. The PCR conditions were: 94°C 2 min; and 30 cycles of 94°C 30 sec, 60°C 1 min, 72°C 1 min and 30 sec.

Semi-quantitative RT-PCR

Total RNA was extracted from seedlings and 6-week-old plants (leaves, stems, roots and flowers) with the RNAeasy Mini Kit (QIAGEN, Valencia, CA). The RNA integrity was verified with formaldehyde agarose gels [109]. First-strand cDNA was synthesized with Superscript II reverse transcriptase (Invitrogen, Carlsbad, CA) using oligodT$_{(18)}$ primer and 2 μg total RNA. Equal amounts of these cDNAs were used as a template in the PCR reactions. Gene-specific primers were used for HMA3 (Forward: 5'-GTCATCGTTCCTTCTAGAACCGTCATC-3'; Reverse: 5'-GGATAAGACCAGCGGGACAACCAC-3'), HMA4 (Forward: 5'-CACCAGTTGCTACTTTCTGTGCAC-3'; Reverse: 5'-CCGGTTTGTTTTTCATCGCTGC-3'), HMA8 (Forward: 5'-AGACTCGCTATTGGTTTTGCCTGG-3'; Reverse: 5'-TTCCAGCTTCACCATGTCCGA-3') and the ubiquitous transcription factor eEF1α (Forward: 5'-AGGAGCCCAAGTTTTTGAAGA-3'; Reverse: 5'-TTCTTCACTGCAGCCTTGGT-3'). The PCR conditions were: 94°C 2 min; 30 cycles of 94°C 15 sec, 55°C 30 sec, 72°C 3 min; and a final extension of 3 min at 72°C. The number of cycles was chosen after an optimization step where 20, 25, 30 and 35 cycles were assayed. In the RT-PCR for T-DNA insertion lines the same PCR conditions were used.

Generation of transgenic plants

Arabidopsis thaliana plants were transformed with *Agrobacterium tumefaciens* holding the construct in pDESTG2 vector by floral dip as previously described [113]. Briefly, *Agrobacterium tumefaciens* strain carrying HMA8 promoter in pDESTG2 vector was grown overnight, spun down and resuspended to OD$_{600}$≈0.8 in 5% sucrose solution. Silwet L-77 (Lehle Seeds, Round Rock, TX) was added to a concentration of 0.05% and

above-ground parts of plant were dipped in the *Agrobacterium* solution for 2 to 3 seconds with gentle agitation. For 24 h the plants were placed under a plastic dome to maintain high humidity and then grown normally. Seeds were harvested, placed in agar selective plates (containing 50 ug/ml Kanamycin), cold treated for 48 h and grown in plant chamber for 7-10 days. Putative transformants plants were then transplanted to soil, grown and checked for the presence of the expression product (GUS activity).

GUS staining

Arabidopsis thaliana transgenic plants showing β-glucurodinase activity under HMA8 promoters were generated. The histochemical assay to screen for the expression of GUS activity was carried out as previously described [114]. Briefly, plant tissue was incubated in the reaction buffer containing 50 mM NaH_2PO_4 pH 7, 0.01 % Tween 20, 10 mM Na_2EDTA, 0.5 mM $K_3Fe(CN)_6$, 0.5 mM $K_4Fe(CN)_6$ and 0.3 % w/v 5-bromo-4-chloro-3-indolyl glucuronide (X-gluc) as a substrate for the enzyme. After incubation overnight at 37°C the tissues were briefly discolored with ethanol and screened for blue staining (GUS activity indicator).

PbTP Cloning

The DNA coding sequence for PbTP from *Aeropyrum pernix* was previously cloned into pBAD-TOPO vector (Invitrogen, Carlsbad, CA) in our laboratory; using specific primers. The sequence was confirmed by automated DNA sequence analysis (Macrogen Inc., Korea).

PbTP expression

E. coli cells transformed with PbTP-pBAD-TOPO were grown in 2XYT media containing 100mg/l ampicillin at 37˚C. Protein expression was induced with 0.02% arabinose at an optical density (OD 600nm) of 0.6. After 3 hours induction at 37˚C, the cells were harvested by centrifugation at 5000xg for 15 min, washed with 25mM Tris-HCl pH 7, 100mM KCl and the pellet stored at -80˚C until further processing. Expression

was detected by immunostaining using specific anti-His (Affinity Bioreagents, CO) antibody after separating the proteins in 15% polyacrilamide SDS-page gel.

PbTP purification

The frozen cells were resuspended in Buffer A (25mM Tris-HCl pH 7, 100mM sucrose, 1mM PMSF) to 0.4g cells/ml and disrupted in a beads beater (6-8 cycles 30sec ON/ 1min OFF). The cell lysates were incubated with 0.02mg/ml DNAse I and 2mM $MgCl_2$ for 30min at 4°C and centrifuged at 9600xg for 30min. Then, the supernatants were ultracentrifuged at 229000xg for 1h. The resulting pellet (membrane enriched fraction) was resuspended in buffer A and the proteins solubilized by gentle stirring for 1h with 0.75% DDM at 4°C. The soluble fraction was separated from the pellet after a new round of ultracentrifugation. PbTP was purified in a Ni-NTA column (Invitrogen, Carlsbad, CA) following the manufacturers' indications. The imidazole was removed by size exclusion chromatography (Sephadex G-25) using buffer B (25mM Tris-HCl pH8, 50mM NaCl, 1mM DTT)

PbTP ATPase activity assays

Metal dependant ATPase activity was measured in 10μg of membrane enriched fractions or 2-2.5μg purified protein for 10 minutes at 75°C. Briefly, the reaction mix contained 50mM Tris-HCl pH7.5 (at room temperature), 3mM $MgCl_2$, 3mM ATP, 400mM NaCl and the indicated amount of metal. For Pb^{+2} determinations, nitrate salts were used instead of chloride ones to avoid $PbCl_2$ precipitation. For purified protein determinations, the reaction also contained 0.01% asolectin and 0.01% DDM. Pi release was measured using the malachite green method as previously described [115].

REFERENCES

1.   Rensing, C., M. Ghosh, and B.P. Rosen, *Families of soft-metal-ion-transporting ATPases.* J. Bacteriol., 1999. 181(19): p. 5891-5897.
2.   Clemens, S., *Molecular mechanisms of plant metal tolerance and homeostasis.* Planta, 2001. 212(4): p. 475-486.
3.   Guerinot, M.L. and D. Eide, *Zeroing in on zinc uptake in yeast and plants.* Curr. Opin. Plant. Biol., 1999. 2(3): p. 244-249.
4.   Paulsen, I.T. and M.H. Saier, Jr., *A novel family of ubiquitous heavy metal ion transport proteins.* J. Membr. Biol., 1997. 156(2): p. 99-103.
5.   Eide, D. and M.L. Guerinot, *Metal ion uptake in eukaryotes.* Asm. News, 1997. 63(4): p. 199-205.
6.   Williams LE, M.R., *P(1B)-ATPases--an ancient family of transition metal pumps with diverse functions in plants.* Trends in Plant Science, 2005. 10(10): p. 491-502.
7.   Fox, T.C. and M.L. Guerinot, *Molecular biology of cation transport in plants.* Ann. Rev. Plant Phys., 1998. 49: p. 669-696.
8.   Guerinot, M.L., *The ZIP family of metal transporters.* Biochim. Biophys. Acta, 2000. 1465(1-2): p. 190-198.
9.   Solioz, M. and C. Vulpe, *CPx-type ATPases: a class of P-type ATPases that pump heavy metals.* Trends Biochem. Sci., 1996. 21(7): p. 237-241.
10.   O'Halloran, T.V. and V.C. Culotta, *Metallochaperones, an intracellular shuttle service for metal ions.* J. Biol. Chem., 2000. 275(33): p. 25057-25060.
11.   Huffman, D.L. and T.V. O'Halloran, *Function, structure, and mechanism of intracellular copper trafficking proteins.* Annu Rev Biochem, 2001. 70: p. 677-701.
12.   Himelblau, E. and R.M. Amasino, *Delivering copper within plant cells.* Curr. Opin. Plant Biol., 2000. 3(3): p. 205-210.
13.   Cellier, M., G. Prive, A. Belouchi, T. Kwan, V. Rodrigues, W. Chia, and P. Gros, *Nramp Defines a Family of Membrane Proteins.* P. Natl. A. Sci. U S A, 1995. 92(22): p. 10089-10093.
14.   Hall, J.L. and L.E. Williams, *Transition metal transporters in plants.* J. Exp. Bot., 2003. 54(393): p. 2601-2613.
15.   Rosenzweig, A.C., *Metallochaperones: bind and deliver.* Chem Biol., 2002. 9(6): p. 673-677.
16.   Rae, T.D., P.J. Schmidt, R.A. Pufahl, V.C. Culotta, and T.V. O'Halloran, *Undetectable intracellular free copper: The requirement of a copper chaperone for superoxide dismutase.* Science, 1999. 284(5415): p. 805-808.
17.   Culotta, V.C., L.W.J. Klomp, J. Strain, R.L.B. Casareno, B. Krems, and J.D. Gitlin, *The Copper Chaperone for Superoxide Dismutase.* J. Biol. Chem., 1997. 272(38): p. 23469-23472.
18.   Sturtz, L.A., K. Diekert, L.T. Jensen, R. Lill, and V.C. Culotta, *A Fraction of Yeast Cu,Zn-Superoxide Dismutase and Its Metallochaperone, CCS, Localize to the Intermembrane Space of Mitochondria.* J. Biol. Chem., 2001. 276(41): p. 38084-38089.

19.	Glerum, D.M., I. Muroff, C. Jin, and A. Tzagoloff, *COX15 Codes for a Mitochondrial Protein Essential for the Assembly of Yeast Cytochrome Oxidase.* J. Biol. Chem., 1997. 272(30): p. 19088-19094.

20.	Beers, J., D.M. Glerum, and A. Tzagoloff, *Purification, Characterization, and Localization of Yeast Cox17p, a Mitochondrial Copper Shuttle.* J. Biol. Chem., 1997. 272(52): p. 33191-33196.

21.	Pufahl, R.A., C.P. Singer, K.L. Peariso, S.J. Lin, P.J. Schmidt, C.J. Fahrni, V.C. Culotta, J.E. Penner-Hahn, and T.V. O'Halloran, *Metal ion chaperone function of the soluble Cu(I) receptor Atx1.* Science, 1997. 278(5339): p. 853-6.

22.	Klomp, L.W.J., S.-J. Lin, D.S.Y. Klausner, Richard D., V.C. Culotta, and J.D. Gitlin, *Identification and Functional Expression of HAH1, a Novel Human Gene Involved in Copper Homeostasis.* J. Biol. Chem., 1997. 272(14): p. 9221-9226.

23.	Mira, H., F. Martinez-García, and L. Peñarrubia, *Evidence for the plant-specific intercellular transport of the Arabidopsis copper chaperone CCH.* Plant J., 2001. 25(5): p. 521-528.

24.	Balandin, T. and C. Castresana, *AtCOX17, an Arabidopsis homolog of the yeast copper chaperone COX17.* Plant Physiol, 2002. 129(4): p. 1852-7.

25.	Cobine, P., W.A. Wickramasinghe, M.D. Harrison, T. Weber, M. Solioz, and C.T. Dameron, *The Enterococcus hirae copper chaperone CopZ delivers copper(I) to the CopY repressor.* FEBS Lett., 1999. 445(1): p. 27-30.

26.	Odermatt, A. and M. Solioz, *Two trans-Acting Metalloregulatory Proteins Controlling Expression of the Copper-ATPases of Enterococcus hirae.* J. Biol. Chem., 1995. 270(9): p. 4349-4354.

27.	Baker-Austin, C., M. Dopson, M. Wexler, R.G. Sawers, and P.L. Bond, *Molecular insight into extreme copper resistance in the extremophilic archaeon 'Ferroplasma acidarmanus' Fer1.* Microbiology, 2005. 151(Pt 8): p. 2637-46.

28.	Banci, L., I. Bertini, R. Del Conte, J. Markey, and F.J. Ruiz-Duenas, *Copper trafficking: the solution structure of Bacillus subtilis CopZ.* Biochemistry, 2001. 40(51): p. 15660-8.

29.	Rosenzweig, A.C., D.L. Huffman, M.Y. Hou, A.K. Wernimont, R.A. Pufahl, and T.V. O'Halloran, *Crystal structure of the Atx1 metallochaperone protein at 1.02 A resolution.* Structure, 1999. 7(6): p. 605-17.

30.	Anastassopoulou, I., L. Banci, I. Bertini, F. Cantini, E. Katsari, and A. Rosato, *Solution structure of the apo and copper(I)-loaded human metallochaperone HAH1.* Biochemistry, 2004. 43(41): p. 13046-53.

31.	Arnesano, F., L. Banci, I. Bertini, D.L. Huffman, and T.V. O'Halloran, *Solution structure of the Cu(I) and apo forms of the yeast metallochaperone, Atx1.* Biochemistry, 2001. 40(6): p. 1528-39.

32.	Ralle, M., S. Lutsenko, and N.J. Blackburn, *X-ray absorption spectroscopy of the copper chaperone HAH1 reveals a linear two-coordinate Cu(I) center capable of adduct formation with exogenous thiols and phosphines.* J Biol Chem, 2003. 278(25): p. 23163-70.

33.	Wimmer, R., T. Herrmann, M. Solioz, and K. Wuthrich, *NMR structure and metal interactions of the CopZ copper chaperone.* J. Biol. Chem., 1999. 274(32): p. 22597-22603.

34. Banci, L., I. Bertini, and R. Del Conte, *Solution structure of apo CopZ from Bacillus subtilis: further analysis of the changes associated with the presence of copper.* Biochemistry, 2003. 42(46): p. 13422-8.

35. Arnesano, F., L. Banci, I. Bertini, S. Ciofi-Baffoni, E. Molteni, D.L. Huffman, and T.V. O'Halloran, *Metallochaperones and metal-transporting ATPases: a comparative analysis of sequences and structures.* Genome Res., 2002. 12(2): p. 255-271.

36. Wernimont, A.K., D.L. Huffman, A.L. Lamb, T.V. O'Halloran, and A.C. Rosenzweig, *Structural basis for copper transfer by the metallochaperone for the Menkes/Wilson disease proteins.* Nature Struct. Biol., 2000. 7(9): p. 766-771.

37. Hung, I.H., R.L.B. Casareno, G. Labesse, F.S. Mathews, and J.D. Gitlin, *HAH1 is a copper-binding protein with distinct amino acid residues mediating copper homeostasis and antioxidant defense.* J. Biol. Chem., 1998. 273(3): p. 1749-1754.

38. Wernimont, A.K., L.A. Yatsunyk, and A.C. Rosenzweig, *Binding of Copper(I) by the Wilson Disease Protein and Its Copper Chaperone.* J. Biol. Chem., 2004. 279(13): p. 12269-12276.

39. Achila, D., L. Banci, I. Bertini, J. Bunce, S. Ciofi-Baffoni, and D.L. Huffman, *Structure of human Wilson protein domains 5 and 6 and their interplay with domain 4 and the copper chaperone HAH1 in copper uptake.* Proc Natl Acad Sci U S A, 2006.

40. Banci, L., I. Bertini, F. Cantini, C.T. Chasapis, N. Hadjiliadis, and A. Rosato, *A NMR study of the interaction of a three-domain construct of ATP7A with copper(I) and copper(I)-HAH1: the interplay of domains.* J Biol Chem, 2005. 280(46): p. 38259-63.

41. Walker, J.M., R. Tsivkovskii, and S. Lutsenko, *Metallochaperone Atox1 transfers copper to the N-terminal domain of the Wilson's disease protein and regulates its catalytic activity.* J Biol Chem, 2002. 23: p. In press.

42. van Dongen, E.M., L.W. Klomp, and M. Merkx, *Copper-dependent protein-protein interactions studied by yeast two-hybrid analysis.* Biochem Biophys Res Commun, 2004. 323(3): p. 789-95.

43. Banci, L., I. Bertini, S. Ciofi-Baffoni, C.T. Chasapis, N. Hadjiliadis, and A. Rosato, *An NMR study of the interaction between the human copper(I) chaperone and the second and fifth metal-binding domains of the Menkes protein.* Febs J, 2005. 272(3): p. 865-71.

44. Walker, J.M., D. Huster, M. Ralle, C.T. Morgan, N.J. Blackburn, and S. Lutsenko, *The N-terminal metal-binding site 2 of the Wilson's Disease Protein plays a key role in the transfer of copper from Atox1.* J Biol Chem, 2004. 279(15): p. 15376-84.

45. Radford, D.S., M.A. Kihlken, G.P. Borrelly, C.R. Harwood, N.E. Le Brun, and J.S. Cavet, *CopZ from Bacillus subtilis interacts in vivo with a copper exporting CPx-type ATPase CopA.* FEMS Microbiol Lett, 2003. 220(1): p. 105-12.

46. Banci, L., I. Bertini, S. Ciofi-Baffoni, R. Del Conte, and L. Gonnelli, *Understanding copper trafficking in bacteria: interaction between the copper transport protein CopZ and the N-terminal domain of the copper ATPase CopA from Bacillus subtilis.* Biochemistry, 2003. 42(7): p. 1939-49.

47.	Larin, D., C. Mekios, K. Das, B. Ross, A.S. Yang, and T.C. Gilliam, *Characterization of the interaction between the Wilson and Menkes disease proteins and the cytoplasmic copper chaperone, HAH1p.* J. Biol. Chem., 1999. 274(40): p. 28497-28504.

48.	Hamza, I., M. Schaefer, L.W. Klomp, and J.D. Gitlin, *Interaction of the copper chaperone HAH1 with the Wilson disease protein is essential for copper homeostasis.* Proc. Natl. Acad. Sci. U S A, 1999. 96(23): p. 13363-13368.

49.	Huffman, D.L. and T.V. O'Halloran, *Energetics of copper trafficking between the Atx1 metallochaperone and the intracellular copper transporter, Ccc2.* J. Biol. Chem., 2000. 275(25): p. 18611-18614.

50.	Strausak, D., M.K. Howie, S.D. Firth, A. Schlicksupp, R. Pipkorn, G. Multhaup, and J.F. Mercer, *Kinetic analysis of the interaction of the copper chaperone Atox1 with the metal binding sites of the Menkes protein.* J Biol Chem, 2003. 278(23): p. 20821-7.

51.	Arnesano, F., L. Banci, I. Bertini, F. Cantini, S. Ciofi-Baffoni, D.L. Huffman, and T.V. O'Halloran, *Characterization of the binding interface between the copper chaperone Atx1 and the first cytosolic domain of Ccc2 ATPase.* J Biol Chem, 2001. 276(44): p. 41365-76.

52.	Ortiz, D.F., T. Ruscitti, K.F. McCue, and D.W. Ow, *Transport of Metal-binding Peptides by HMT1, A Fission Yeast ABC-type Vacuolar Membrane Protein.* J. Biol. Chem., 1995. 270(9): p. 4721-4728.

53.	Salt, D.E. and W.E. Rauser, *MgATP-Dependent Transport of Phytochelatins Across the Tonoplast of Oat Roots.* Plant Physiol., 1995. 107(4): p. 1293-1301.

54.	Yamaguchi, H., N.-K. Nishizawa, H. Nakanishi, and S. Mori, *IDI7, a new iron-regulated ABC transporter from barley roots, localizes to the tonoplast.* J. Exp. Bot., 2002. 53(369): p. 727-735.

55.	van der Zaal, B.J., L.W. Neuteboom, J.E. Pinas, A.N. Chardonnens, H. Schat, J.A.C. Verkleij, and P.J.J. Hooykaas, *Overexpression of a Novel Arabidopsis Gene Related to Putative Zinc-Transporter Genes from Animals Can Lead to Enhanced Zinc Resistance and Accumulation.* Plant Physiol., 1999. 119(3): p. 1047-1056.

56.	Williams, L.E., J.K. Pittman, and J.L. Hall, *Emerging mechanisms for heavy metal transport in plants.* Biochim. Biophys. Acta, 2000. 1465(1-2): p. 104-126.

57.	Persans, M., K. Nieman, and D.E. Salt, *Functional activity and role of cation-efflux family members in Ni hyperaccumulation in Thlaspi goesingense.* Proc. Natl. Acad. Sci. U S A, 2001. 98(17): p. 9995-10000.

58.	Eide, D., M. Broderius, J. Fett, and M.L. Guerinot, *A novel iron-regulated metal transporter from plants identified by functional expression in yeast.* Proc. Natl. Acad. Sci. U S A, 1996. 93(11): p. 5624-5628.

59.	Korshunova, Y.O., D. Eide, W.G. Clark, M.L. Guerinot, and H.B. Pakrasi, *The IRT1 protein from Arabidopsis thaliana is a metal transporter with a broad substrate range.* Plant Mol. Biol., 1999. 40(1): p. 37-44.

60.	Henrique, R., J. Jasik, M. Klein, E. Martinoia, U. Feller, J. Schell, M.S. Pais, and C. Koncz, *Knock-out of Arabidopsis metal transporter gene IRT1 results in iron deficiency accompanied by cell differentiation defects.* Plant Mol. Biol., 2002. 50(4-5): p. 587-597.

61. Vert, G., N. Grotz, F. Dedaldechamp, F. Gaymard, M.L. Guerinot, J.F. Briat, and C. Curie, *IRT1, an Arabidopsis transporter essential for iron uptake from the soil and for plant growth.* Plant Cell, 2002. 14(6): p. 1223-1233.

62. Grotz, N., T. Fox, E. Connolly, W. Park, M.L. Guerinot, and D. Eide, *Identification of a family of zinc transporter genes from Arabidopsis that respond to zinc deficiency.* Proc. Natl. Acad. Sci. U S A, 1998. 95(12): p. 7220-7224.

63. Wintz, H., T. Fox, Y.-Y. Wu, V. Feng, W. Chen, H.-S. Chang, T. Zhu, and C. Vulpe, *Expression Profiles of Arabidopsis thaliana in Mineral Deficiencies Reveal Novel Transporters Involved in Metal Homeostasis.* J. Biol. Chem., 2003. 278(48): p. 47644-47653.

64. Thomine, S., R. Wang, J.M. Ward, N.M. Crawford, and J.I. Schroeder, *Cadmium and iron transport by members of a plant metal transporter family in Arabidopsis with homology to Nramp genes.* Proc. Natl. Acad. Sci. U S A, 2000. 97(9): p. 4991-4996.

65. Curie, C., J.M. Alonso, M. Le Jean, J.R. Ecker, and J.F. Briat, *Involvement of NRAMP1 from Arabidopsis thaliana in iron transport.* Biochem. J., 2000. 347(3): p. 749-755.

66. Thomine, S., F. Lelievre, E. Debarbieux, J.I. Schroeder, and H. Barbier-Brygoo, *AtNRAMP3, a multispecific vacuolar metal transporter involved in plant responses to iron deficiency.* Plant J., 2003. 34(5): p. 685-695.

67. Cohen, C.K., T.C. Fox, D.F. Garvin, and L.V. Kochian, *The role of iron-deficiency stress responses in stimulating heavy-metal transport in plants.* Plant Physiol., 1998. 116(3): p. 1063-1072.

68. Portnoy, M.E., X.F. Liu, and V.C. Culotta, *Saccharomyces cerevisiae expresses three functionally distinct homologues of the Nramp family of metal transporters.* Molecular and Cellular Biology, 2000. 20(21): p. 7893-7902.

69. Glynn, I.M., *The Na^+,K^+-transporting adenosine triphosphatase.*, in *Enzymes of Biological Membranes*, A. Martonosi, Editor. 1985, Plenum PL: New York. p. 35-114.

70. Kaplan, J.H., *Biochemistry of Na,K-ATPase.* Ann. Rev. Biochem., 2002. 71: p. 511-535.

71. Jorgensen, P.L. and J.P. Andersen, *Structural basis for E1-E2 conformational transitions in Na, K-pump and Ca-pump proteins.* J. Mem. Biol., 1988. 103: p. 95-120.

72. MacLennan, D.H., W.J. Rice, and N.M. Green, *The mechanism of Ca^{2+} transport by sarco(endo)plasmic reticulum Ca^{2+}-ATPases.* J. Biol. Chem., 1997. 272(46): p. 28815-28818.

73. Sweadner, K.J. and C. Donnet, *Structural similarities of Na,K-ATPase and SERCA, the Ca2+-ATPase of the sarcoplasmic reticulum.* Biochem. J., 2001. 356: p. 685-704.

74. Toyoshima, C., M. Nakasako, H. Nomura, and H. Ogawa, *Crystal structure of the calcium pump of sarcoplasmic reticulum at 2.6 Å resolution.* Nature, 2000. 405(6787): p. 647-655.

75. Toyoshima, C. and H. Nomura, *Structural changes in the calcium pump accompanying the dissociation of calcium.* Nature, 2002. 418(6898): p. 605-11.

76.   Axelsen, K.B. and M.G. Palmgren, *Evolution of substrate specificities in the P-type ATPase superfamily.* J. Mol. Evol., 1998. 46(1): p. 84-101.

77.   Palmgren, M.G. and K.B. Axelsen, *Evolution of P-type ATPases.* Biochim. Biophys. Acta, 1998. 1365(1-2): p. 37-45.

78.   Rensing, C., B. Mitra, and B.P. Rosen, *The zntA gene of Escherichia coli encodes a Zn(II)-translocating P-type ATPase.* Proc. Natl. Acad. Sci. U S A, 1997. 94(26): p. 14326-14331.

79.   Sharma, R., C. Rensing, B.P. Rosen, and B. Mitra, *The ATP hydrolytic activity of purified ZntA, a Pb(II)/Cd(II)/Zn(II)-translocating ATPase from Escherichia coli.* J. Biol. Chem., 2000. 275(6): p. 3873-3878.

80.   Mandal, A.K. and J.M. Argüello, *Functional roles of metal binding domains of the Archaeoglobus fulgidus Cu(+)-ATPase CopA.* Biochemistry, 2003. 42(37): p. 11040-11047.

81.   Mandal, A.K., W.D. Cheung, and J.M. Argüello, *Characterization of a thermophilic P-type Ag+/Cu+-ATPase from the extremophile Archaeoglobus fulgidus.* J. Biol. Chem., 2002. 277(9): p. 7201-7208.

82.   Mana-Capelli, S., A.K. Mandal, and J.M. Argüello, *Archaeoglobus fulgidus CopB Is a Thermophilic Cu^{2+}-ATPase: Functional Role of Its Histidine-rich N-terminal Metal Binding Domain.* J. Biol. Chem., 2003. 278(42): p. 40534-40541.

83.   Lutsenko, S. and J.H. Kaplan, *Organization of P-type ATPases: Significance of structural diversity.* Biochemistry, 1995. 34(48): p. 15607-15613.

84.   Argüello, J.M., *Identification of ion selectivity determinants in heavy metal transport P1B-ATPases.* J. Mem. Biol., 2003. 195: p. 93-108.

85.   Yoshimizu, T., H. Omote, T. Wakabayashi, Y. Sambongi, and M. Futai, *Essential Cys-Pro-Cys motif of Caenorhabditis elegans copper transport ATPase.* Biosci. Biotechnol. Biochem., 1998. 62(6): p. 1258-1260.

86.   Lutsenko, S. and M.J. Petris, *Function and Regulation of the Mammalian Copper-transporting ATPases: Insights from Biochemical and Cell Biological Approaches.* J. Mem. Biol., 2002. 191(1): p. 1-12.

87.   Argüello, J.M. and J.H. Kaplan, *Glutamate 779, an intramembrane carboxyl, is essential for monovalent cation binding by the Na,K-ATPase.* J. Biol. Chem., 1994. 269(9): p. 6892-6899.

88.   Ogawa, H. and C. Toyoshima, *Homology modeling of the cation binding sites of Na+K+-ATPase.* Proc. Natl. Acad. Sci. U S A, 2002. 99(25): p. 15977-15982.

89.   Tsivkovskii, R., B. MacArthurs, and S. Lutsenko, *The Lys(1010)-Lys(1325) fragment of the Wilson's disease protein binds nucleotides and interacts with the N-terminal domain of this protein in a copper-dependent manner.* J. Biol. Chem., 2001. 276(3): p. 2234-2242.

90.   Voskoboinik, I., D. Strausak, M. Greenough, H. Brooks, M. Petris, S. Smith, J.F. Mercer, and J. Camakaris, *Functional analysis of the N-terminal CXXC metal-binding motifs in the human Menkes copper-transporting P-type ATPase expressed in cultured mammalian cells.* J. Biol. Chem., 1999. 274(31): p. 22008-22012.

91.   Mitra, B. and R. Sharma, *The cysteine-rich amino-terminal domain of ZntA, a Pb(II)/Zn(II)/Cd(II)-translocating ATPase from Escherichia coli, is not essential for its function.* Biochemistry, 2001. 40: p. 7694-7699.

92. Bal, N., E. Mintz, F. Guillain, and P. Catty, *A possible regulatory role for the metal-binding domain of CadA, the Listeria monocytogenes Cd^{2+}-ATPase.* FEBS Lett., 2001. 506(3): p. 249-252.

93. Abdel-Ghany, S.E., P. Muller-Moule, K.K. Niyogi, M. Pilon, and T. Shikanai, *Two P-Type ATPases Are Required for Copper Delivery in Arabidopsis thaliana Chloroplasts.* Plant Cell, 2005. 17(4): p. 1233-1251.

94. Shikanai, T., P. Muller-Moule, Y. Munekage, K.K. Niyogi, and M. Pilon, *PAA1, a P-Type ATPase of Arabidopsis, Functions in Copper Transport in Chloroplasts.* Plant Cell, 2003. 15(6): p. 1333-1346.

95. Tabata, K., S. Kashiwagi, H. Mori, C. Ueguchi, and T. Mizuno, *Cloning of a cDNA encoding a putative metal-transporting P-type ATPase from Arabidopsis thaliana.* Biochim Biophys Acta, 1997. 1326(1): p. 1-6.

96. Hirayama, T., J.J. Kieber, N. Hirayama, M. Kogan, P. Guzman, S. Nourizadeh, J.M. Alonso, W.P. Dailey, A. Dancis, and J.R. Ecker, *RESPONSIVE-TO-ANTAGONIST1, a Menkes/Wilson disease-related copper transporter, is required for ethylene signaling in Arabidopsis.* Cell, 1999. 97(3): p. 383-393.

97. Woeste, K.E. and J.J. Kieber, *A strong loss-of-function mutation in RAN1 results in constitutive activation of the ethylene response pathway as well as a rosette-lethal phenotype.* Plant Cell, 2000. 12(3): p. 443-455.

98. Andres-Colas, N., V. Sancenon, S. Rodriguez-Navarro, S. Mayo, D.J. Thiele, J.R. Ecker, S. Puig, and L. Penarrubia, *The Arabidopsis heavy metal P-type ATPase HMA5 interacts with metallochaperones and functions in copper detoxification of roots.* Plant J, 2006. 45(2): p. 225-36.

99. Gravot, A., A. Lieutaud, F. Verret, P. Auroy, A. Vavasseur, and P. Richaud, *AtHMA3, a plant P_{1B}-ATPase, functions as a Cd/Pb transporter in yeast.* FEBS Lett., 2004. 561(1-3): p. 22-28.

100. Mills, R.F., G.C. Krijger, P.J. Baccarini, J.L. Hall, and L.E. Williams, *Functional expression of AtHMA4, a P1B-type ATPase of the Zn/Co/Cd/Pb subclass.* Plant J., 2003. 35(2): p. 164-176.

101. Hussain, D., M.J. Haydon, Y. Wang, E. Wong, S.M. Sherson, J. Young, J. Camakaris, J.F. Harper, and C.S. Cobbett, *P-type ATPase heavy metal transporters with roles in essential zinc homeostasis in Arabidopsis.* Plant Cell, 2004. 16(5): p. 1327-39.

102. Eren, E. and J.M. Arguello, *Arabidopsis HMA2, a divalent heavy metal-transporting P(IB)-type ATPase, is involved in cytoplasmic Zn2+ homeostasis.* Plant Physiol, 2004. 136(3): p. 3712-23.

103. Cobbett, C.S., D. Hussain, and M.J. Haydon, *Structural and functional relationships between type 1B heavy metal-transporting P-type ATPases in Arabidopsis.* New Phytol., 2003. 159: p. 315-321.

104. Mandal, A.K., Y. Yang, T.M. Kertesz, and J.M. Arguello, *Identification of the transmembrane metal binding site in Cu+ transporting PIB-type ATPases.* J. Biol. Chem., 2004: p. M410854200.

105. Verret, F., A. Gravot, P. Auroy, N. Leonhardt, P. David, L. Nussaume, A. Vavasseur, and P. Richaud, *Overexpression of AtHMA4 enhances root-to-shoot translocation of zinc and cadmium and plant metal tolerance.* FEBS Lett, 2004. 576(3): p. 306-12.

106. Colangelo, E.P. and M.L. Guerinot, *Put the metal to the petal: metal uptake and transport throughout plants.* Curr Opin Plant Biol, 2006.

107. Mills, R.F., G.C. Krijger, P.J. Baccarini, J.L. Hall, and L.E. Williams, *Functional expression of AtHMA4, a P1B-type ATPase of the Zn/Co/Cd/Pb subclass.* Plant J, 2003. 35(2): p. 164-76.

108. Hou, Z. and B. Mitra, *The metal specificity and selectivity of ZntA from Escherichia coli using the acylphosphate intermediate.* J Biol Chem, 2003. 278(31): p. 28455-61.

109. Sambrook, J., E.F. Fritsch, and T. Maniatis, *Molecular cloning. A laboratory Manual.* 1989, New York: Cold Spring Harbor Laboratory Press.

110. Bradford, M.M., *A rapid and sensitive method for the quantitation of microgram quantities of protein utilizing the principle of protein-dye binding.* Anal. Biochem., 1976. 72: p. 248-254.

111. Laemmli, U.K., *Cleavage of structural proteins during the assembly of the head of bacteriophage T4.* Nature, 1970. 227(259): p. 680-685.

112. Edwards, K., C. Johnstone, and C. Thompson, *A simple and rapid method for the preparation of plant genomic DNA for PCR analysis.* Nucleic Acids Res., 1991. 19(6): p. 1349.

113. Clough, S. and A. Bent, *Floral dip: a simplified method for Agrobacterium-mediated transformation of Arabidopsis thaliana.* Plant J., 1998. 16(6): p. 735-743.

114. Jefferson, R.A., T.A. Kavanagh, and M.W. Bevan, *GUS fusions betaglucuronidase as a sensitive and versitle gene fusion marker in higher plants.* EMBO J., 1987. 6: p. 3901-3907.

115. Lanzetta, P.A., L.J. Alvarez, P.S. Reinach, and O.A. Candia, *An improved assay for nanomole amounts of inorganic phosphate.* Anal. Biochem., 1979. 100(1): p. 95-97.